# African Journal of Engineering Research and Innovation

AJERI Vol 2. No. 1. 2024

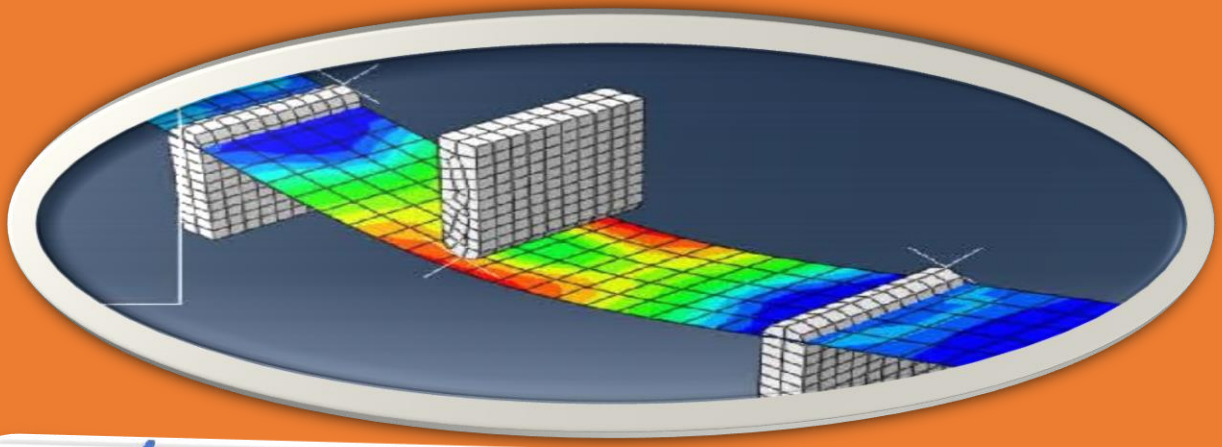

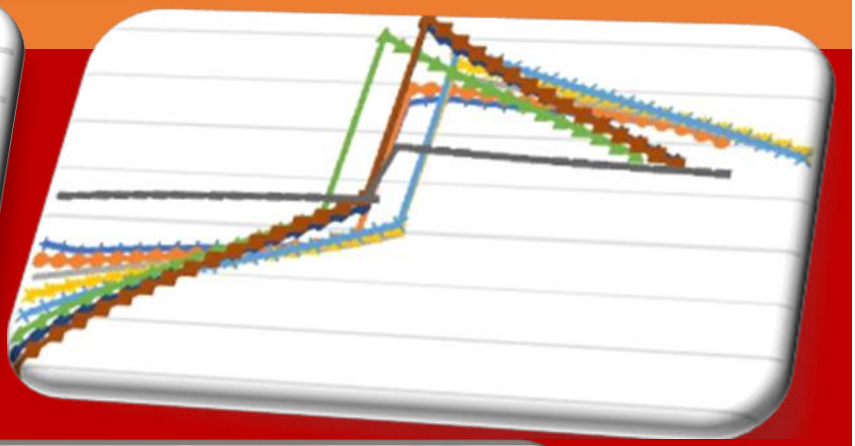

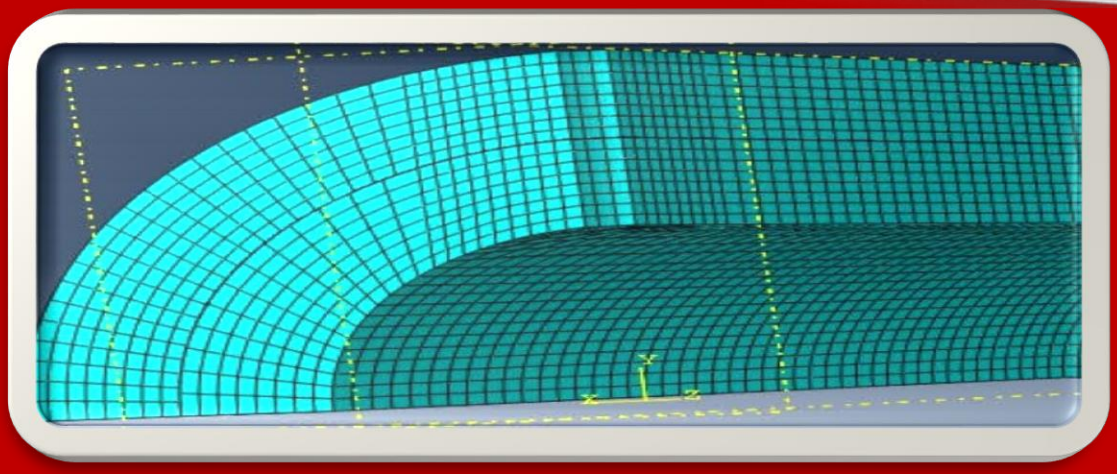

## The Institution of Engineers of Kenya

ISSN: 2957- 7780

# In partnership with

# AJERI

## *African Journal of Engineering in Research and Innovation*

ISSN: 2957- 7780 Volume 2. No 1. 2024

Published by:

The *Institution of Engineers of Kenya*

P.O Box 41346- 00100

Nairobi Kenya

Tel: +254 (20) 2729326, 0721 729363, (020) 2716922

Email: editor@iekenya.org

Website: www.iekenya.org

**IEK**

**African Journal of Engineering Research and Innovation (AJERI),** is published by **The *Institution of Engineers of Kenya,*** IEK, as an international forum for publication of high-quality papers in all areas of Engineering

**CONTENTS** **Pages**

# Design and Implementation of Remote Surface Electromyography Monitoring System for Patients with Muscle Disorders

N. K. Mutai[1], M. O. Odhiambo[2], E. W. Mukubwa[1]

[1]Moi University, Eldoret, Kenya, [2]Mangosuthu University of Technology, Durban, South Africa.

**Abstract**

Remote electromyography monitoring systems have emerged as a valuable tool in the field of healthcare. Wearable surface electromyography monitoring systems have the potential to provide continuous and objective monitoring of muscle activity in patients with muscle disorders. This paper presents a wearable surface electromyography monitoring system that consists of electromyography sensors, transmission unit and a processing unit which utilize Internet of Things. The system is capable of acquiring and processing surface electromyography signals from biceps muscles simultaneously and providing real-time feedback on muscle activity patterns allowing patients to carry out their daily activities without interference. The proposed system has the potential to improve the diagnosis of patients with muscle disorders.

**Keywords** - surface electromyography, muscles disorder, remote monitoring, real-time notifications, sensors, GPS/GSM communication

## 1. Introduction

For patients with muscular disorders such as muscular dystrophy, myasthenia gravis, or amyotrophic lateral sclerosis, surface electromyography monitoring systems can be particularly useful. These conditions are characterized by muscle weakness, wasting, and degeneration, which can lead to difficulties with mobility, breathing, and other activities of daily living. Surface electromyography monitoring systems can provide clinicians with an objective measure of muscle activity and function, which can be used to tailor treatment plans and monitor disease progression. In addition to clinical applications, remote surface electromyography monitoring systems also have the potential to improve patient self-management and quality of life.

By providing patients with access to real-time muscle activity data, these systems can help patients to better understand their condition, track their progress, and make informed decisions about their treatment and lifestyle choices. Furthermore, remote monitoring can reduce the need for in-person clinic visits, which can be particularly beneficial for patients who live in remote or underserved areas.

Wearable sensors have increasingly been incorporated and used in the rehabilitation of patients who suffer from diseases with associated movement restrictions. The advantage here is that wearable sensors provide real-world data on patients' movement performance. Wearable sensors are used in various contexts, both for monitoring purposes at home and in community settings. Applications focus on the assessment of treatment efficacy, early detection of disorders, prevention and home rehabilitation as well as the provision of an input variable for the control of prostheses and assistive systems such as robots and intelligent orthoses. Quantitative measures enable the assessment of treatment efficacy and are an important tool with which clinicians can tailor therapy to the individual needs of their patients as they provide information about the patients' performance between two therapeutic sessions. This not only allows remote monitoring by the therapist but can also give direct feedback to the patient.

## 2. Literature Review

A significant portion of the global population suffers from muscular diseases, which is a widespread health problem. These ailments frequently cause the muscles' capacity to contract and relax to be impaired, which lowers the patient's functional ability. An essential tool for identifying and tracking muscular illnesses is surface electromyography (surface electromyography), a non-invasive method that measures the electrical activity of muscles. Traditional surface electromyography monitoring methods, however, need that patients go to a clinic or hospital, which can be both expensive and difficult in remote areas. Additionally, because these devices only record the patient's muscle activity in a single moment, it is challenging to track improvements over time.

Smart sensors are typically used in wearable technology to identify different bodily factors and prompt the user or caregiver to take the proper action [1,2]. Wearable medical devices have emerged as a result of improvements in mobile technology and the growing demand from an older population for healthcare management [3,4,5]. These devices allow people to monitor their personal health information in real time. Because of the capability of constant monitoring, diseases can be prevented and urgent health problems can be avoided. Currently, a large number of wearable healthcare devices offer body bio-signals for diagnosis, including electroencephalograms, electrocardiograms (ECGs), blood glucose levels, body temperature, and electromyograms (EMGs) [6,7,8]. ECG and EMG measurements, which are brought on by changes in electrical signal during muscular activity, are significant and often utilized metrics for healthcare management.

Electrocardiography involves applying electrodes to the skin to capture the electrical activities of the beating heart muscles over time [9]. The electro physiologic pattern-the heart muscle depolarizing and repolarizing during each heartbeat-produces the minor electrical change on the skin, which is

produced and detected by an ECG signal detection device. The ECG signal detection system is being developed in the direction of miniaturization, family, and intelligence in response to the growing awareness of people's health and the ongoing advancement of science and technology. For precise ECG monitoring while exercising, Sun et al. inserted conductive fabric ECG electrodes into a health shirt [10].

Another electro diagnostic medical tool is electromyography, which measures and records the muscular electrical signal produced by skeletal muscle activities [11]. When muscle cells are stimulated by electricity or nerves, muscle potentials can result. As a result, it is possible to identify and assess human biomechanics, medical problems, or activation level [12]. EMG signal analysis has recently been used in medical and healthcare applications [14,15]. Benatti et al. suggested an adaptable integrated architecture for EMG acquisition for gesture recognition [15].

The current electromyography tests done in Kenyan Neurological hospitals are short-lasting and it is confined in a limited laboratory space since they are wired and non-remote. And these tests are done by few hospitals making it hard to access the service easily. Most use needle electrodes which are invasive, uncomfortable and intolerable to patients. Requires regular visits to neurologist and booking of appointments are required. All this makes the whole system expensive. For example, Nairobi Neurocare hospital charges Kshs. 20,000 to perform a single EMG test. The absence of efficient and trustworthy remote monitoring capabilities for surface electromyography systems, which restricts their usage for patients who require long-term monitoring or who live in rural or underserved locations, is thus the issue that the surface electromyography remote monitoring system attempts to address. The creation of a dependable and user-friendly remote monitoring system for surface electromyography has the potential to promote research into the health and function of muscles as well as patient care and outcomes for those with muscular illnesses. Consequently, take into account the shortcomings of the present system. In comparison to invasive EMG systems, remote EMG monitoring systems have a number of benefits, including improved convenience, mobility, cost-effectiveness, data quality, patient participation, and efficiency. They also address the problem of staff inadequacy in Kenya. To conclude, this project will be a great achievement in telemedicine field in Kenya particularly remote monitoring in remote areas. We have used the cheapest components.

## 3. Methodology

Remote monitoring device will consist of both hardware and software components which will be integrated together to accomplish the task.

### Hardware Components

NodeMCU -This is a powerful development board based on the ESP8266 chip, which allows for easy integration of Wi-Fi functionality into electronic projects. The board can be powered via micro USB or through an external power supply connected to the VIN pin. The NodeMCU can communicate the processed signals and output to other devices, such as my laptop, through various communication protocols such as USB or Wi-Fi. The NodeMCU will transmit Surface Electromyography (surface electromyography) data to ThingSpeak and via GSM module to a phone. I preferred NodeMCU board due to its built-in Wi-Fi capabilities, powerful microcontroller, high customizability, and affordability. Its ability to connect to the internet and transmit data wirelessly is essential for transmitting EMG data to the cloud-based IoT platform. Its powerful microcontroller and Lua programming language allow for efficient data processing, while its customizability enables developers to add custom functionalities and integrate various sensors and modules. Additionally, its affordability and availability make it accessible to a wide range of users, including healthcare professionals, researchers, and caregivers.

**Power Supply**- The proposed system will be supplied by two 9V batteries connected in series. The surface electromyography sensor will be directly connected to this power supply while the other components will be powered by 5V power supply from a buck converter. A Buck Converter can be used to power a NodeMCU (which operates at 5V) by converting a 18V to 5V required by the NodeMCU. The Buck Converter can regulate the voltage and ensure a stable and consistent power supply to the NodeMCU. The NodeMCU produces 3.3V by using its onboard voltage regulator. The voltage regulator is responsible for converting 5V to the required voltage for the NodeMCU and its peripheral devices. This 3.3V will power GSM and GPS module.

**GSM Module** -SIM800L is a quad-band GSM/GPRS module that operates on the frequencies of 850MHz, 900MHz, 1800MHz, and 1900MHz. It communicates with microcontrollers via serial communication and requires a minimum of four connections ($V_{CC}$, GND, RX, TX). The NodeMCU will send the processed surface electromyography data to a phone via a GSM module (SIM800L) by establishing a mobile connection and sending a text message. The NodeMCU will use an appropriate library or API to interface with the GSM module and send the data. If the internet connection fails, the 2G capabilities of GSM will still function to send the data.

**EMG Sensors**- A sensor is a transducer device to detect events or changes in its environment, and then provide a corresponding electrical output. The most important characteristics of a sensor are precision, resolution, linearity, and speed. Figure. 1 shows the Surface EMG v3 sensor is a type of electromyography (EMG) sensor that is used to measure the electrical activity of skeletal muscles.

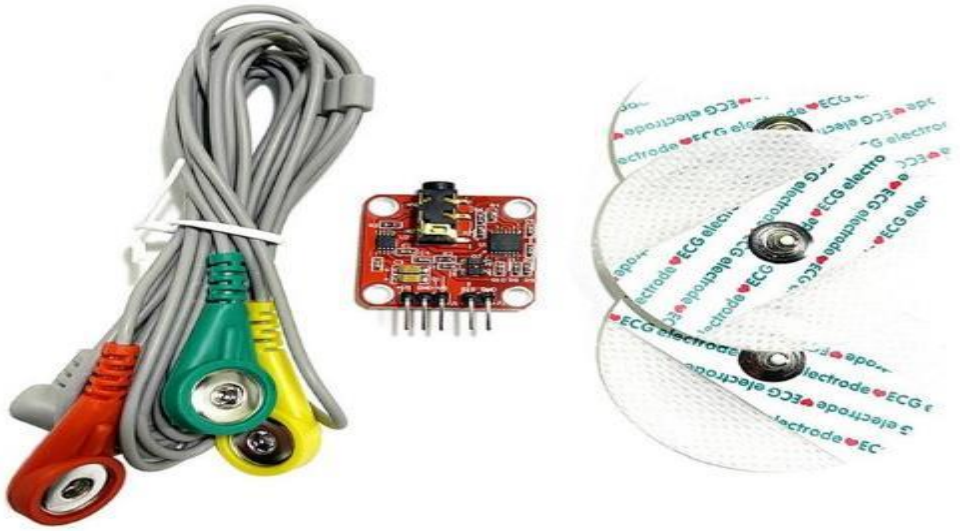

*Figure 1: EMG V3 Sensor with Electrodes*

The sensor works by detecting the electrical signals that are generated by muscle fibers when they contract. The Surface EMG v3 sensor consists of three electrodes that are placed on the skin surface above the muscle of interest. Two electrodes serve as the recording electrode, while the other electrode serves as the reference electrode. The recording electrodes detects the electrical signals generated by the muscle fibers, while the reference electrode provides a stable reference point for the measurement. The two electrodes on the belly of the biceps muscle serve as the recording electrodes and detect the electrical signals generated by the muscle fibers during contraction. The reference electrode provides a stable reference point against which the electrical activity of the biceps muscle can be measured. The output signals can then be processed and analysed by a NodeMCU microcontroller. Surface EMG electrodes provide a non-invasive technique for measurement and detection of EMG signal. These electrodes are simple and very easy to implement. Gelled electrodes are preferred over Dry electrodes due to its light weight reducing problems of electrode fixation Encountered when using dry electrodes.

**GPS Module** - The NEO-6M GPS module is a compact, low-power GPS receiver with high accuracy and fast time-to-first-fix. It communicates with microcontrollers via serial communication and requires a minimum of four connections ($V_{CC}$, GND, RX, TX). It will provide precise locations as needed.

**Software**

**Arduino IDE** (Integrated Development Environment) is an open-source software development platform designed for programming Arduino boards. Arduino IDE is used to write, compile, and upload code to Arduino boards, which can be used for a wide range of applications such as robotics, home automation, Internet of Things (IoT), and many more. The IDE includes a code editor with

features such as syntax highlighting, code completion, and error highlighting. It also includes a library manager with a wide range of pre-built libraries that can be easily added to the code. The serial monitor in the IDE allows for real-time monitoring of the input and output of the Arduino board. Arduino IDE will be used to write, compile, and upload code to the NodeMCU development board.

**ThingSpeak** : The NodeMCU will be programmed to send the processed surface electromyography data to ThingSpeak, an IoT platform, using the ThingSpeak API. The NodeMCU establishes a secure connection with ThingSpeak and sends the data in a specific format. In order for the results to be send and displayed on a web site, the system was linked to thingspeak.com web server, a site that supports Internet of Things (IoT) developers to post and manipulate their data for visualization.
SYSTEM DESIGN

The software design for this project involves several components that need to be developed and integrated together to achieve the desired functionality. The main components include the NodeMCU firmware, EMG data processing algorithm, ThingSpeak integration, GSM module integration, GPS module integration, and threshold checking algorithm. Below is a block diagram of how the whole system will work. Figure 2 shows how EMG electrode sensors will detect muscle activities. They will continuously monitor muscle activities present as electric potential generated by muscle cells when they are electrically or neurologically activated.

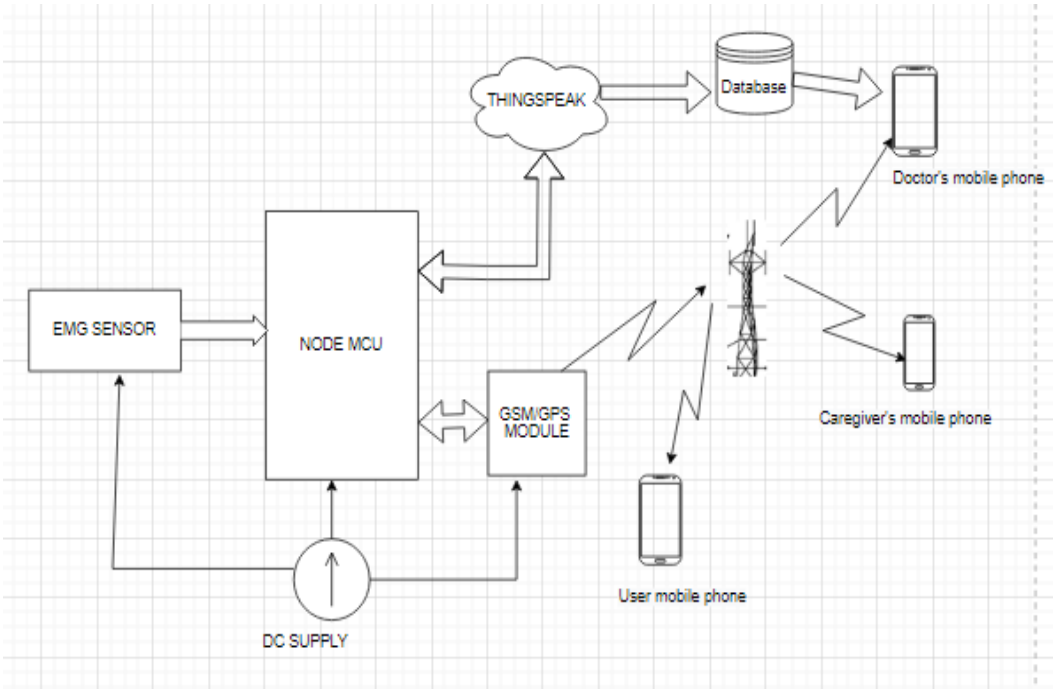


*Figure 2: Block Diagram of Remote surface electromyography monitoring system*

NodeMCU is responsible for reading data from the EMG v3 sensor, processing the data to obtain meaningful information, setting thresholds, and sending data to ThingSpeak and the GSM module.

The data is then stored in ThingSpeak channels for further analysis and visualization by the doctor. The GPS coordinates are sent to GSM module when the muscle activity level exceeds the threshold.

The threshold checking algorithm was integrated into the EMG data processing algorithm and the NodeMCU firmware. The algorithm compares the RMS value of the EMG signal to a pre-defined threshold and determines if the muscle activity level is within a normal range or if it has exceeded the threshold. If the threshold is exceeded, the algorithm triggers the GSM module to send SMS messages containing the GPS coordinates. The circuit diagram as shown in Figure 3.

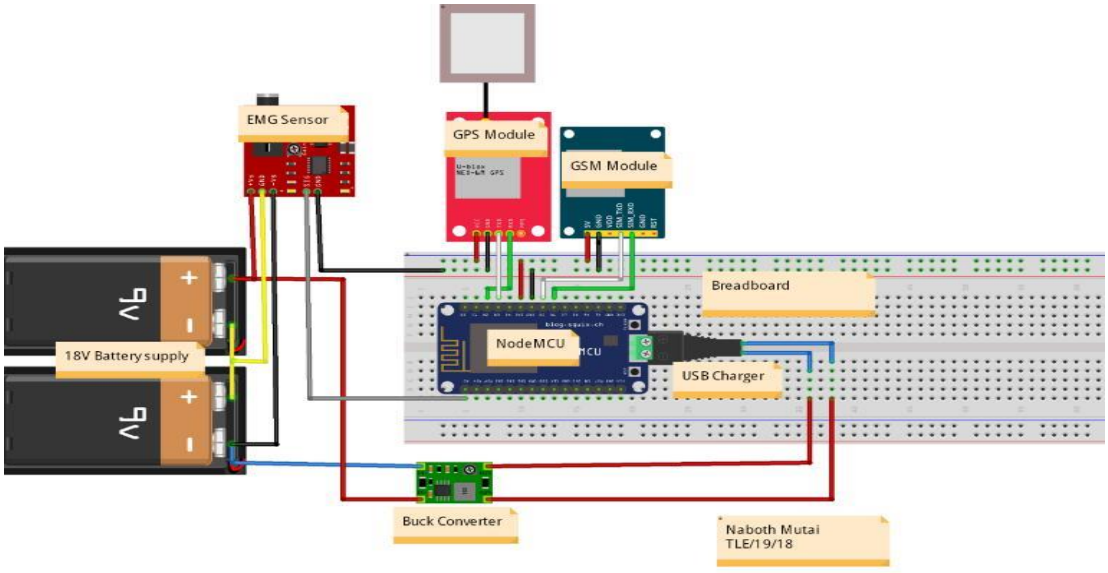


*Figure 3: Circuit Diagram of Remote surface electromyography monitoring system*

Figure 4 represents the flowchart of operations of the surface electromyography Remote monitoring, showing each step with various conditions. The process starts with collection of EMG data, processing them to be sent via WiFi and GSM module, it checks if there's WiFi connection, this process repeats until the connection is made, during the internet connection process, GSM will sent the readings to the phone.

After this threshold is checked, if exceeded GPS is activated to obtain its coordinates and alert messages with GPS coordinates are sent. The process is repeated sequentially.

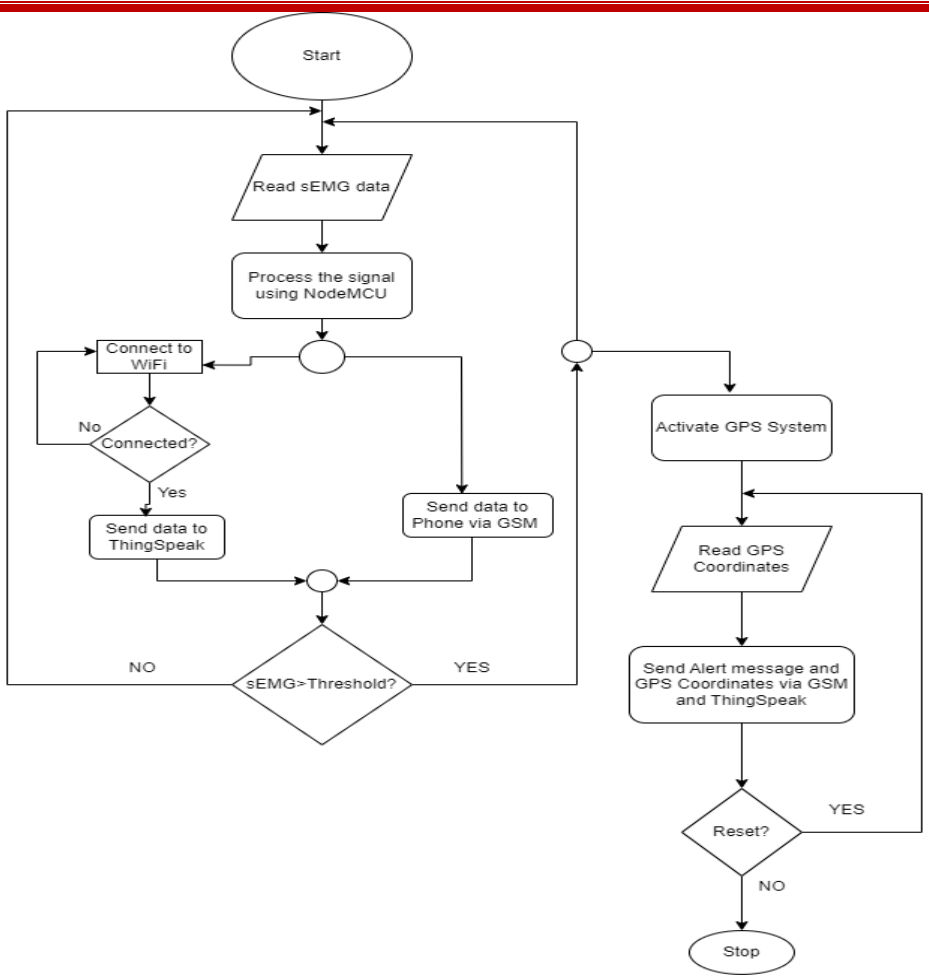


*Figure 4: Flowchart of operations of the of surface electromyography Remote monitoring system*

## 4. IMPLEMENTATION

The prototype or experimental setup is depicted in Figure 5. This system has been tested by placing the surface electrodes on a human body for reference, detection and ground junction.

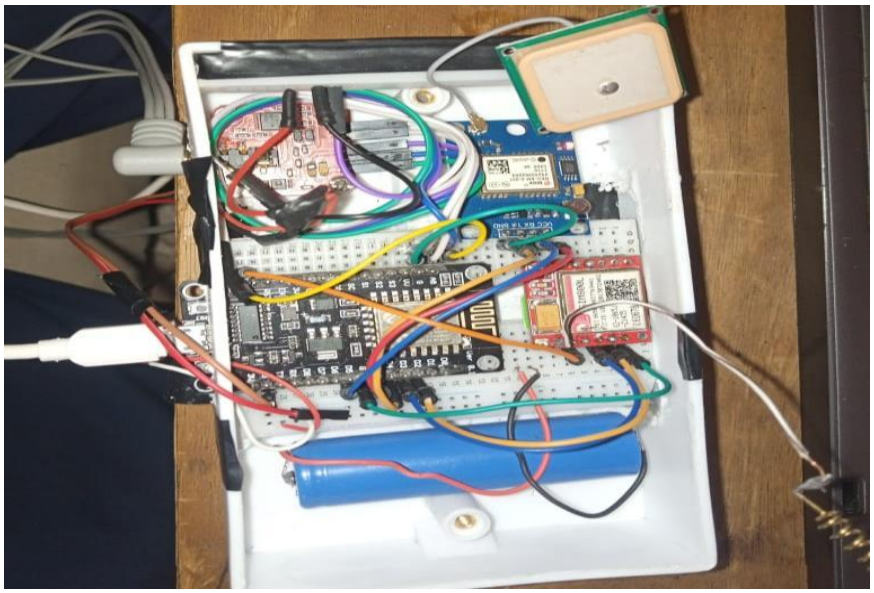

*Figure 5: Prototype of the surface electromyography monitoring system*

Figure 6 shows the placement of electrodes on the biceps brachii muscles. These electrodes are connected to the EMG sensor module which is then powered up to start collected data. The procedure was conducted based on Weiss guide on Performing Nerve Conduction Studies and Electromyography [13].

*Figure 6: Electrode placement during testing*

When the EMG sensor is interfaced with the NodeMCU then after compiling and building the code which also configures the ThingSpeak server, real-time EMG readings can be monitored. This implementation thus utilizes the concept of IoT. The EMG monitoring signal is displayed on the Cloud as shown in Figure 7 depicts visual representation of EMG data that was collected and uploaded to ThingSpeak. This provides a valuable insights into the electrical activity of skeletal muscles that can be used by the doctor to analyse muscle activation patterns.

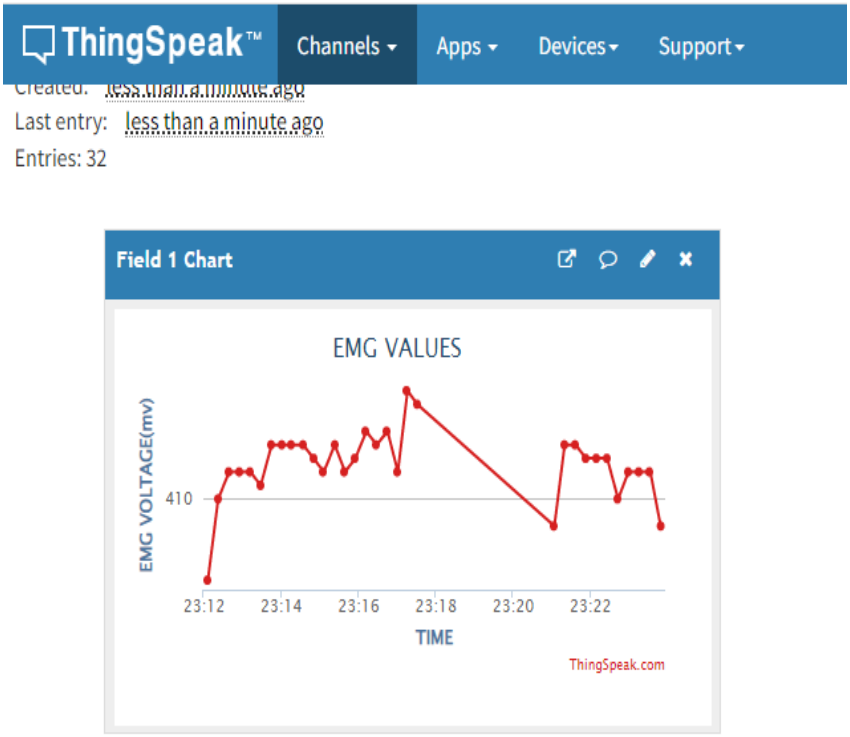


*Figure 7: ThingSpeak EMG charts*

The same data was sent via WiFi to the cloud was also sent to my phone using GSM module, sample EMG data was received as shown in Figure 8. In remote areas where internet connectivity is limited, GSM will still transmit the data from EMG sensor to the doctor's phone. This makes the system suitable for monitoring in remote locations.

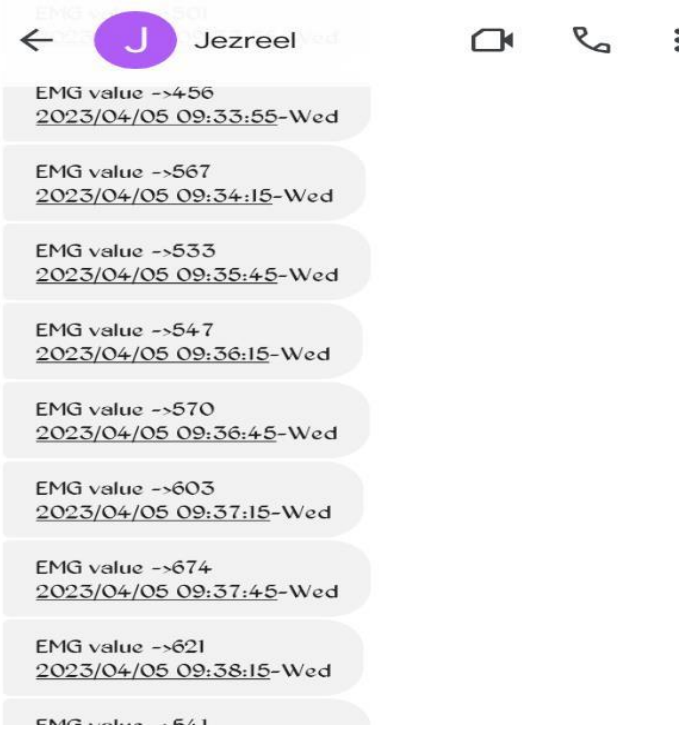


*Figure 8: Sample EMG data received from GSM module*

After doing a vigorous muscle exercise, threshold was exceeded and alert messages with GPS locations were also sent to phone as SMS messages as shown in Figure 9.

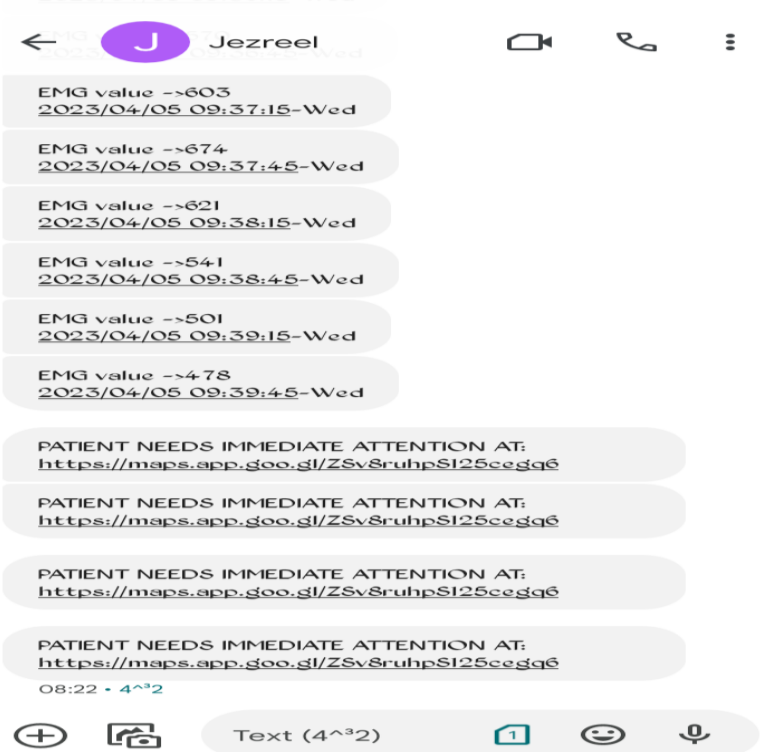


*Figure. 9: Alert Messages with location link*

## 5. Conclusions

The project successfully achieved its objectives, as evidenced by the successful implementation of each of the project's steps, from collecting EMG data to transmitting it to the ThingSpeak platform and mobile phone. A simple prototype of remote health monitoring system was developed using NodeMCU which was capable of transmitting data through WiFi and GSM module via SMS. The System was able to transmit data to a web server through the ESP8266 WIFI module. It was also able to send data to a mobile phone via SMS and relay an alert message with GPS coordinates when threshold values were exceeded.

## References

[1] Soh, P.J.; Vandenbosch, G.A.E.; Mercuri, M.; Schreurs, D.M.M.P. Wearable Wireless Health Monitoring: Current Developments, Challenges, and Future Trends. *IEEE Microw. Mag.* **2015**, *16*, 55–70

[2] Guk, K.; Han, G.; Lim, J.; Jeong, K.; Kang, T.; Lim, E.-K.; Jung, J. Evolution of Wearable Devices with Real-Time Disease Monitoring for Personalized Healthcare. *Nanomaterials* **2019**, *9*, 813.

[3] Wearable Technology Applications in Healthcare: A Literature Review. Available online: **https://www.himss.org/resources/wearable-technology-applications-healthcare-literature-review**

[4] Helbostad, J.; Vereijken, B.; Becker, C.; Todd, C.; Taraldsen, K.; Pijnappels, M.; Aminian, K.; Mellone, S. Mobile health applications to promote active and healthy ageing. *Sensors* **2017**, *17*, 622.

[5] Lee, J.-W.; Yun, K.-S. ECG Monitoring Garment Using Conductive Carbon Paste for Reduced Motion Artifacts. *Polymers* **2017**, *9*, 439.

[6] Kim, J.; Campbell, A.S.; de Avila, B.E.; Wang, J. Wearable biosensors for healthcare monitoring. *Nat. Biotechnol.* **2019**, *37*, 389–406

[7] Reilly, R.B.; Lee, T.C. Electrograms (ECG, EEG, EMG, EOG). *Technol. Health Care* **2010**, *18*, 443–458.Li, J.; Igbe, T.; Liu, Y.; Nie, Z.; Qin, W.; Wang, L.; Hao, Y. An Approach for Noninvasive Blood Glucose Monitoring Based on Bioimpedance Difference Considering Blood Volume Pulsation. *IEEE Access* **2018**, *6*, 51119–51129.

[8] Jung, H.C.; Moon, J.H.; Baek, D.H.; Lee, J.H.; Choi, Y.Y.; Hong, J.S.; Lee, S.H. CNT/PDMS composite flexible dry electrodes for long-term ECG monitoring. *IEEE Trans. Biomed. Eng.* **2012**, *59*, 1472–1479

[9] Li, W.; Zhang, H.; Wan, J.; Li, Y. A wearable exercise heart rate detection device based on single-arm ECG. In Proceedings of the International Conference on Biological Information and Biomedical Engineering (BIBE 2018), Shanghai, China, 6–8 June 2018; pp. 1–4.

[10] Sun, F.; Yi, C.; Li, W.; Li, Y. A wearable H-shirt for exercise ECG monitoring and individual lactate threshold computing. *Comput. Ind.* **2017**, *92*, 1–11

[11] ] Lapkova, D.; Kralik, L.; Adámek, M. EMG analysis for basic self-defense techniques. In *Computer Science On-Line Conference*; Springer: Cham, Switzerland, 2016; pp. 353–362.

[12] Ali, A.A. EMG signals detection technique in voluntary muscle movement. In Proceedings of the 2012 6th International Conference on New Trends in Information Science, Service Science and Data Mining (ISSDM2012), Taipei, Taiwan, 23–25 October 2012; pp. 738–742..

[13] Weiss, L.D.; Weiss, J.M.; Silver, J.K. Easy EMG E-Book: A Guide to Performing Nerve Conduction Studies and Electromyography, 2nd ed.; Elsevier: Amsterdam, The Netherlands, 2015

[14] Zulkifli, A.; Ummu, J.K.; Aishah, A.F.Q.A.; Najeb, J.M. Development of wearable electromyogram (EMG) device for upper extremity in aerobic exercise. *IOP Conf. Ser. Mater. Sci. Eng.* **2019**, *469*, 012085

[15] Benatti, S.; Casamassima, F.; Milosevic, B.; Farella, E.; Schonle, P.; Fateh, S.; Burger, T.; Huang, Q.; Benini, L. A Versatile Embedded Platform for EMG Acquisition and Gesture Recognition. *IEEE Trans. Biomed. Circuits Syst.* **2015**, *9*, 620–63

# Contribution of 3D model representation in subsurface geotechnical investigations

F. Ng'eno*, C. Omuto and E. Biamah

Department of Environmental and Biosystems Engineering, University of Nairobi

P.O. Box 30197-00100, Nairobi, Kenya

**Abstract**

3D model representation is important in enhancing geotechnical site characterization. It was initially widely used in geologic investigations. Due to its increasing demand in geotechnical engineering, there has been an upsurge in its application in subsurface investigations. Similarly, more dedicated software are being developed to support application demands. This study reviewed progress of 3D modelling in geotechnical investigations including current practices and opportunities for improvement. It showed that 3D modelling of geotechnical investigations has been popularly used in subsurface risk assessment, visualization, and identification of important target sections or occurrence of resources such as quarry materials, groundwater, or hard stratum. These applications are supported by numerous standalone software or add-on computer scripts or packages. However, most software are still lacking some important functionalities such as uncertainty assessment. Independent computer scripts seem to break this limitation but still need more improvements and wide application. An example of this application was shown in a case study in Mombasa Kenya, where 3D modelling potential was used to identify weak subsurface sections, 3D visualization, and identification of groundwater in a project site for construction of an inland container depot.

*Keywords:* ***software, 3D model, geotechnical investigations, data processing***

## 1. Introduction

Geotechnical investigation is normally carried out to assess site suitability for construction of a proposed project. It helps to determine the strength and behaviour of the ground and construction materials and to analyze potential risks to the proposed construction (Bo, 2022; Look, 2007). Subsurface investigation focuses on uncovering buried characteristics beneath the surface through inversive methods (such as drilling, excavation trenches/pits, etc.) or non-inversive methods such as sounding s or a combination of both methods (Hunt, 2007). Inversive methods provide direct actual

measurements or observations in narrow openings through the subsurface profile. They also allow subsurface sampling for further laboratory testing and analysis. Hence, they are traditionally preferred even though they are cumbersome and cover only limited discrete points in a proposed project site (Longoni et al., 2012). This article illustrates how they have been or can be enriched to improve their representation of geotechnical properties of a construction site.

Methods for subsurface geotechnical investigations have evolved over the years. The most prominent old technique was the digging of pits and trenches to access soil and rock features below the surface (Griffiths, 2014; Hool and Kinne, 1923). This method was improved by the advent of the drilling technology. This technology improved the efficiency and depth of digging in response to the increasing demand for space for urban growth, infrastructure development, resource exploration, and waste disposal (Brady et al., 2017; Reiffsteck et al., 2018). Instrumented and smart drilling have further improved the drilling technology (Alqadad et al., 2017). Furthermore, integrated application of drilling technology and non-inversive methods such as geophysical sounding and remote sensing have made tremendous improvements in subsurface investigations (Devi et al., 2017; Sulistijo and Anwar, 2013). There are still challenges with data handling that is commensurate with advances in equipment for subsurface investigations. This study reviewed opportunities for data handling to improve subsurface characterization of geotechnical properties.

Subsurface geotechnical investigations are not without challenges. The challenges often encountered include inaccurate equipment, heterogeneity of target site, presence of underground utilities (e.g., pipes, electrical lines, etc.), variable fill material, groundwater flow, weather conditions, and site access and safety (Otake and Honjo, 2022; Zhang, 2011). There are also data challenges particularly in sample selection prior to investigation, data mining, and visualization of the final investigation outcome. Data handling challenges are also observable in situations involving integrated use of different equipment, equipment generating large data, and time-series data (El Sibaii et al., 2022, 2022). Recent developments in building information modelling (BIM), GIS, and statistical modelling software have helped to improve efficient and accurate geotechnical data handling (Bui et al., 2016). This paper reviewed advancements in geotechnical investigation data representation with particular focus on three-dimension (3D) data management.

Inversive subsurface geotechnical investigations are mostly given in one-dimensional (1D) representation known as borehole log. The log shows properties of soil and rock materials down the vertical profile (Hunt, 2007; Wang et al., 2022). Although 1D representation of geotechnical investigations is reliable because it contains primary observations/measurements at the sampled locations, it does not show spatial variations between observation points in a project site. Subsurface geotechnical conditions in most project site are naturally varied, which require many spatially located observation locations for adequate characterization (Caballero et al., 2022). Geographic Information System (GIS), geostatistics and non-inversive investigation methods have been used to overcome the limitations of 1D borehole logs (Awan et al., 2022; Liu et al., 2023; Orhan and Tosun, 2010). These 2D approaches have a better representation of spatial variations of geotechnical properties. They can portray spatial variations either in a vertical plane (such as in cross-sections) or horizontally across the landscape. Three or more dimensional visualization is the ultimate representation since it combines both vertical and horizontal dimensions in one illustration (Dong et al., 2015; Hack et al., 2006; Petrone et al., 2023). This paper analyzed the potential of 3D modelling in subsurface geotechnical investigations.

## 2. 3D Modelling Of Geotechnical Investigations

Three-dimensional representation of geotechnical investigations is an illustration of a volumetric cross-section of the target site. It should show 2D variations of the geotechnical properties in an x-y plane either at each sampling depth (Figure 1a) or at each sampling transect (Figure 1b). The 3D model is an ensemble of the 2D maps in a project site (Figure 1c). Different approaches have been proposed in the literature for developing 2D maps and 3D models.

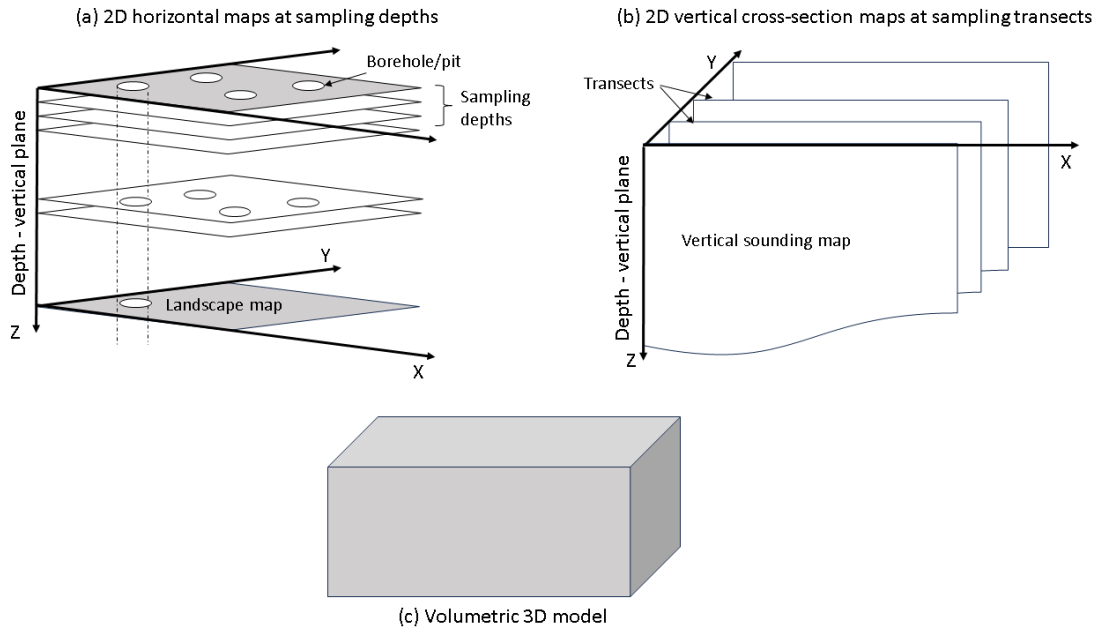


Figure 1: Concept of 3D model for subsurface geotechnical investigations

*2.1 Approaches for 2D maps of subsurface geotechnical investigations*

2D map of geotechnical properties gives a cross-sectional slice of the subsurface. The slice is either vertical down the profile or horizontal across the landscape (Figure 1). The vertical cross-section produces a snapshot of subsurface stratigraphy from top (surface) to the bottom. This type of cross-section is mostly produced by the geophysical sounding approach (Azrief Azahar et al., 2019; Romero-Ruiz et al., 2018; Tsai and Lin, 2022) or series of borehole/excavation pits a long a transect line (Guan and Wang, 2021) (Table 1). Geophysical approach uses electric, magnetic, sonic, radio, or seismic signals to determine orientation, depth, and geotechnical characteristics of earth materials within range of the signals. The signals are either emitted and recorded by specialized instrument(s) or are naturally emitted from the earth and recorded by the instruments (Chandran and Anbazhagan, 2017). 2D vertical cross-sections are used to determine orientation and depth of subsurface strata, location of cavities or variation in strength of subsurface strata, thickness of strata, potential underground hazards to construction project, changes in geotechnical properties with subsurface depth, among others (Medhus and Klinkby, 2023; Paillet and Saunders, 1990; Soupios et al., 2007). They are also suitable for evaluating risk to existing foundations. Despite their importance in subsurface characterization, vertical cross-sections are limited to the transect line or excavation boreholes/pits in which they are developed. Resultant maps from the cross-

section are assumed as representative of the entire project site, which can be a source of uncertainty when characterizing the entire construction site.

Table 1: Approaches for 2D mapping of subsurface geotechnical characteristics

| **Cross -section** | **Approach** | **Techniques** | **Reference** |
|---|---|---|---|
| Vertical | Geophysical sounding | Seismic | (Bačić et al., 2020) |
| | | Potential (Gravity, electric, magnetic, etc) | (Dezert et al., 2019) |
| | | Electromagnetic | (Auken et al., 2017) |
| | | Sonic | (McNally, 1990) |
| | Drilling/Excavation | Borehole, Pit excavation | (Hunt, 2007) |
| Horizontal | Drilling and GIS | Geostatistics | (Pinheiro et al., 2018) |
| | Remote sensing | Satellite | (Chen et al., 2016) |
| | | Ground Penetrating Radar | (Siggins, 1990) |
| | | Electromagnetic Induction | (Pellerin, 2002) |

The horizontal cross-section of the subsurface portrays a stratum layer at a given depth. It's produced by mapping spatial distribution of many observations in the project site or through remote sensing techniques such as satellites, aerial photographs, and proximal sensing (Table 1) (Liu et al., 2016; Von Hebel et al., 2014). Most Geographic Information System (GIS) approaches depict this type of cross-section when they map geotechnical properties of the site at a given depth. This approach uses geostatistical methods to integrate observations at discrete locations to produce maps of the geotechnical properties (Ahmed et al., 2020; Aldefae et al., 2020; El-Banna et al., 2023; Labib and Nashed, 2013).

### *2.2 Approaches for 3D model for subsurface geotechnical investigations*

A 3D model for geotechnical investigations endeavors to integrate both vertical and horizontal cross-sections of a project site into a volumetric solid representation of subsurface geotechnical conditions. It's increasingly being demanded in geotechnical investigations since it portrays a complete subsurface ground condition more than 1D or 2D representations (Kahlström et al., 2021; Petrone et al., 2023). Three approaches are available in the literature for developing 3D models for geotechnical investigations: 1) modelling of geotechnical interfaces, 2) fusion of 2D layers in a GIS, and 3) three-dimensional geotechnical objects (Table 2).

Table 2: Approaches for 3D modelling of geotechnical investigations

| **Approach** | **Method** | **Reference** |
|---|---|---|
| Geomodelling of geotechnical interfaces | Surface mesh generation | (Frank et al., 2007) |
| | Planar mesh and interpolation | (Mallet, 1997) |
| Fusion of 2D layers | Machine learning | (S. Wu et al., 2021) |
| | Geostatistics and GIS | (Kim et al., 2020) |
| | Sequential gaussian simulation | (Aghamolaie et al., 2019) |
| | Finite element | (Hemeda, 2019) |
| 3D geotechnical objects | Building Information Model | (Satyanaga et al., 2023) |
| | Wireframe and voxel | (Moore and Johnson, 2001) |
| | Intersection of triangulated surfaces | (Elsheikh and Elsheikh, 2014) |
| | Volumetric solid model | (Lemon and Jones, 2003) |

Approaches such as geo-modelling of geotechnical interfaces and building of 3D geotechnical objects are mostly geological methods popularly used by geologists in large projects. They have been used in large-scale hydrogeologic frameworks for groundwater, geologic hazards, mineral exploration, etc. (X. Wu et al., 2021). (Ozmutlu and Hack, 2006) have also shown their application in feasibility studies for subsurface stability in landslide-prone areas. However, they are not so popular in geotechnical engineering especially in small projects and where input geotechnical observations are few (Mei, 2014). Moreover, they are currently not adequately amenable to uncertainty analysis. Approaches involving fusion of model elements are the most popular in small-scale geotechnical investigations. They have been applied successfully in small and large projects alike since they integrate geological modelling approaches with GIS and geostatistics of geotechnical observations and discrete locations (De Rienzo et al., 2008; Masoud et al., 2022). Since they include statistical methods, they can also be used to develop uncertainty analysis of the 3D model.

All approaches for 3D modelling of geotechnical investigations involve aspects of data acquisition, data preparation and processing, model testing, and model application (El Sibaii et al., 2022). These four-stage processes differ with geotechnical investigation projects. However, if they are harmonized and standardized then they can be a useful input into the Building Information Modelling (BIM) paradigm. BIM paradigm proposes

digital collection and sharing of geotechnical and construction information of projects (Eastman et al., 2018; El Sibaii et al., 2022). Presently, there are no clear standards and harmonization procedures in BIM to support its extension to geotechnical investigations and 3D modelling (Valeria et al., 2019). An initial step to create strategies for BIM-like information management and data-sharing of geotechnical information would be the development of proper data management. This has been observed in the literature and proposition of software for kickstarting the process (Hamman et al., 2017; Lee et al., 1990; Montanari and Previatello, 1979).

## 3. Software for 3D Modelling

Development of software for modelling geotechnical investigations was originally motivated by the programming progress in the mining and gas exploration sectors. The first attempt of computer aided investigations was an adaptation of the then mining software, which opened the way for more customization (Orlić, 1997). These attempts were mainly software capable of developing 1D or 2D models. The main challenges to quick development of dedicated software for 3D models for geotechnical investigations were: 1) lack of adequate understanding and detailed data for subsurface geotechnical characteristics, 2) demand for geotechnical investigations was still nascent, and 3) there were few experts to mount such a trivial demand (Toll and Barr, 2001). Progress was made with development of software based on finite element method, which is limited in robust characterization of variations of geotechnical properties in vertical and horizontal dimensions. The software have been documented in geotechnical and geo-environmental software directory[1]. Some of these are shown in Table 3, which shows that they are mostly commercially available.

Table 3: Software for 3D modelling of geotechnical investigations

| **Software** | **Visualization** | **License** | **site characterization** | **Other functionality** | **Company** |
|---|---|---|---|---|---|
| Subsurface analyst | yes | Commercial | Yes | | |
| Vulcan explore bundle | yes | Commercial | | | |
| WLD 3D visualizer | yes | Commercial | | | |
| Slide 3D | yes | Commercial | | Numerical modelling | Rocscience |

[1] http://www.ggsd.com/, accessed on 23 October 2023

| Software | Visualization | License | site characterization | Other functionality | Company |
|---|---|---|---|---|---|
| Plaxis 3D | yes | Commercial | Yes | Numerical modelling | Seequent |
| RS3 | yes | Commercial | yes | Numerical modelling | Rocscience |
| Adina | | Commercial | | Numerical modelling | |
| Adonis | yes | Open-source | | Numerical modelling | |
| Diana finite element analysis | yes | Commercial | Yes | Numerical modelling | Diana FEA |
| Irazu | | Commercial | | Numerical modelling | Geomechanica |
| Midas GTS NX | | Commercial | | Numerical modelling | Midas IT |
| GEMS | | Commercial | | Numerical modelling | GEMS |
| TatukGIS | | Commercial | | Numerical modelling | Tatuk GIS |
| CESAR-LCPC | yes | Commercial | | Numerical modelling | Itech |
| Versat-P3D | | Commercial | | Numerical modelling | |
| Leapfrog Works | yes | Commercial | | Data management | Seequent |
| Oasis montaj | yes | Commercial | | Data management | Seequent |
| Res3DInv | | Commercial | | Data management | Seequent |
| HoleBase | yes | Commercial | | Data management | Seequent |
| Geo5 | yes | Commercial | Yes | Engineering geology | Fine Software |
| GST | yes | Commercial | | Data management | GiGa infosystem |
| Map3D | yes | Commercial | Yes | | Mine Modelling Pty Ltd |
| Stress Transform | | Open-source | | Stress calculation | |
| AutoCAD Civil 3D | yes | Commercial | | Design | Autodesk |

Recently, open-source platforms and computer packages have been developed to support wide program or computer script development. They include GIS software, statistical software, and numerical modelling software. They have facilitated the development of numerous add-on packages and open-source scripts for most computer applications in geo-environmental engineering sectors. For example, GemPy, which is a python script, has shown tremendous applications in 3D modelling of subsurface geologic

investigations (De La Varga et al., 2019). (Bullejos et al., 2022) also developed a python code for 3D visualization of borehole strata using borehole logs. Many more python scripts have since been produced for soil and rock properties, albeit with focus on geology or groundwater characterization (Rasmussen, 2020; Schorpp et al., 2022).

## 4. Application Of 3D Models in Geotechnical Investigations

### *4.1. Risk assessment*

Geotechnical investigations for risk assessment can be taken either before or after construction of a project or foundation. Most assessments done before construction have limited restrictions compared to those carried out after construction. 3D models play crucial role in portraying volumetric representation of the subsurface conditions by locating the orientation and magnitude of risk factors such as fault lines, hollow sections, weak strata, presence of utility lines, groundwater potential, etc. They are also suitable in forensic projects where restrictions and precisions are involved. (Marache et al., 2009) used 3D modelling to show infrastructure damage due to differential settlement in France. (Liu et al., 2021)used it to develop geo-hazard monitoring and early warning in China. (Venmans et al., 2015) used 3D modelling approach in the Netherlands to map geotechnical risk for infrastructural works in Deltaic area.

Most applications for risk assessment use dedicated 3D software for geotechnical and geologic modelling. There are very few cases in literature where independent or add-on scripts have been used although they have potential. The scripting approach may be more robust given that they are amenable to manipulation to suit changing characteristics of risk assessment demands. The scripts can be used to integrate geophysical methods and limited drilling to produce the 3D models. (Cueto et al., 2018) used this approach to map subsurface karst sinkholes in Saudi Arabia. The same approach was also used by (Arisona et al., 2020) to map subsurface voids in Kinta Valley in Malaysia.

In the risk assessment applications, 3D models are used to locate depth of the risk from the soil surface and the distance to the construction/foundation. The models also show extent of the risk and danger it poses to the construction.

### *4.2 Visualization*

3D models of geotechnical investigations give a realistic representation of actual orientation of the subsurface characteristics than 1D or 2D models. Hence, they are most

suitable where subsurface complexity cannot be adequately represented by 1D or 2D. Through 3D visualization, it is possible to view neighborhood relationships and total number of strata in a project subsurface (Guo et al., 2021). This is particularly important in areas where there is demand for subsurface space utilization and limited land space for horizontal expansion for infrastructure development. In such cases, 3D visualization gives more clarity of available and suitable underground space for expansion of structural development. There are many examples in the literature which have demonstrated these applications. For example, (De Rienzo et al., 2008) used 3D to improve visualization of subsurface characteristics in underground civil planning in Turin, Italy. (He et al., 2023) used 3D visualization to show stratigraphic distribution of a subsurface in Tongzhou in China. A similar approach was also used by (Masoud et al., 2022) to improve visualization of subsurface for urban planning in Medina, Saudi Arabia.

### *4.3 Location of target points*

Geotechnical investigations facilitate identification of target sites and volume of resources such as groundwater, rock, minerals, quarry materials, etc. 3D model helps to illustrate multi-dimensional aspects of these characteristics to improve subsequent engineering designs where they are involved. For example, 3D model can adequately illustrate the depth and extent of hard layers when designing pile foundation (Priya and Dodagoudar, 2017; Touch et al., 2014). Its application in the mining industry has been well practiced over the years (Akiska, 2013; Kaufmann and Martin, 2008). They have also been extensively used in hydrogeologic exploration of groundwater occurrence and impact of groundwater fluctuation to foundation stability (Beygi et al., 2020; Mielby and Sandersen, 2017). (Vanneschi et al., 2014) used 3D modelling in excavation activities such as determination of volume of quarry material at a proposed site.

Although there are successful applications of 3D modelling in the literature for locating subsurface target site and volume of resources, there is no clear information of how these applications incorporate uncertainty analysis. Most applications use software or methods that overlook the importance of uncertainty analysis in the 3D models. It is important to incorporate this aspect into the applications to improve confidence and accuracy of subsequent utilization of the application results.

*4.4 Example case study in Mombasa Kenya*

3D geotechnical model was developed for a construction project in Kibarani Inland Container depot in Mombasa County in Kenya (Figure 2). 32 boreholes were drilled using motorized percussion driller and standardized penetrometer test (SPT) according to ASTM D1586 procedure. The project site was initially used as a municipal waste dumping area for more than 30 years. Hence, the top layers were mainly waste material and had to be removed upto 15 m to 20 m prior to geotechnical testing.

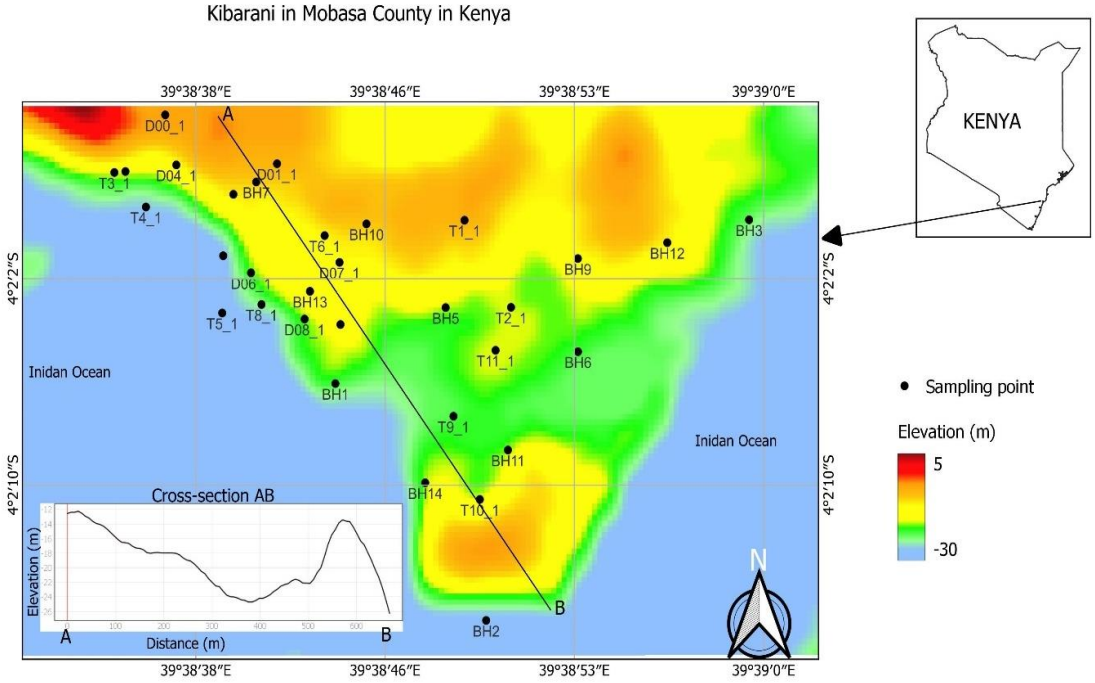


Figure 2: Construction project site

*4.5. Data collection*

Geotechnical investigations were carried out by drilling georeferenced boreholes (Figure 1) and carrying out in-situ testing (Standard Penetrometer Test (SPT) and vane shear test) and sampling for laboratory analysis of Atterberg limits (liquid and plastic limits). The tests and sampling were carried out on soil material at irregular depth intervals up to the rock restriction. SPT was carried out according to ASTM D1586/D1586M-18e1 and vane shear test according to ASTM D2573-08 standards. Samples for laboratory analyses were collected using the split barrel on the SPT equipment (Hunt, 2007). Liquid limit (LL) and plastic limit (PL) tests were done according to ASTM D4318. SPT test produced number of blows (SPT-N) to push the rod to penetrate 15 cm into the soil, vane shear test

produced undrained shear resistance in $kN/m^2$, and Atterberg limits test produced liquid and plastic limits (Table 4).

**Table 4:** Range of values of soil properties from geotechnical site investigation

| No. | Depth (m) | SPT-N (blows) | Resistance ($kN/m^2$) | Liquid limit (LL) (%) | Plastic limit (PL) (%) |
|---|---|---|---|---|---|
| 1 | 1 - 11 | 3 - 30 | 33 - 101 | 22 - 48 | 13.6 - 34.7 |
| 2 | 2.5 - 13.6 | 5 - 32 | 38 - 121 | 27 - 64.2 | 12 - 33.9 |
| 3 | 4.5 - 22 | 5 - 32 | 38 - 133 | 27 - 50 | 12 - 33.9 |
| 4 | 10 - 28 | 15 - 37 | 45 - 189 | 25 - 44 | 13 - 30 |

SPT counts in boreholes were recorded at 1, 2, 5, 10, 15, 20, 25, and 30 m below the surface. These depth intervals were standardized to ensure uniform intervals for all boreholes in the project site. The tests were used to develop 3D model and show model's importance in risk assessment, visualization, and determination of presence of groundwater which may impact foundation design. 3D model was developed using a computer script written in R (R Core team, 2023). Risk assessment targeted presence of weak layers (low SPT Counts) within the subsurface. They are expected to cause uneven settlement that can cause foundation failure. Visualization targeted stratigraphic orientation of the subsurface to identify suitable areas that can be used to support different foundation designs.

The 3D model showed that shoreline areas had rather weak soil/rock material that may not support high stress foundation (Figure 3). The central parts of the site also seem to portray weak subsurface strata and fractured rocks. Borehole logs around these areas showed groundwater presence between 19m and 23 m below the surface. The northern parts and southern tip undulating into the Indian Ocean seem to have relatively deep soil with strong strata. There was no groundwater presence in these parts. Analysis of uncertainty showed that the areas with high SPT counts had relatively higher uncertainties than those with low SPT counts (Figure 4). This implies that even though the northern and southern parts of the project site are relatively strong, there may be local weak points that should be looked for during the design or construction. On the other hand, the central areas have high probability of bearing weak strata and should be targeted for low stress foundation applications. Uncertainty analysis in Figure 4 also shows that the top strata were more varied than the bottom strata.

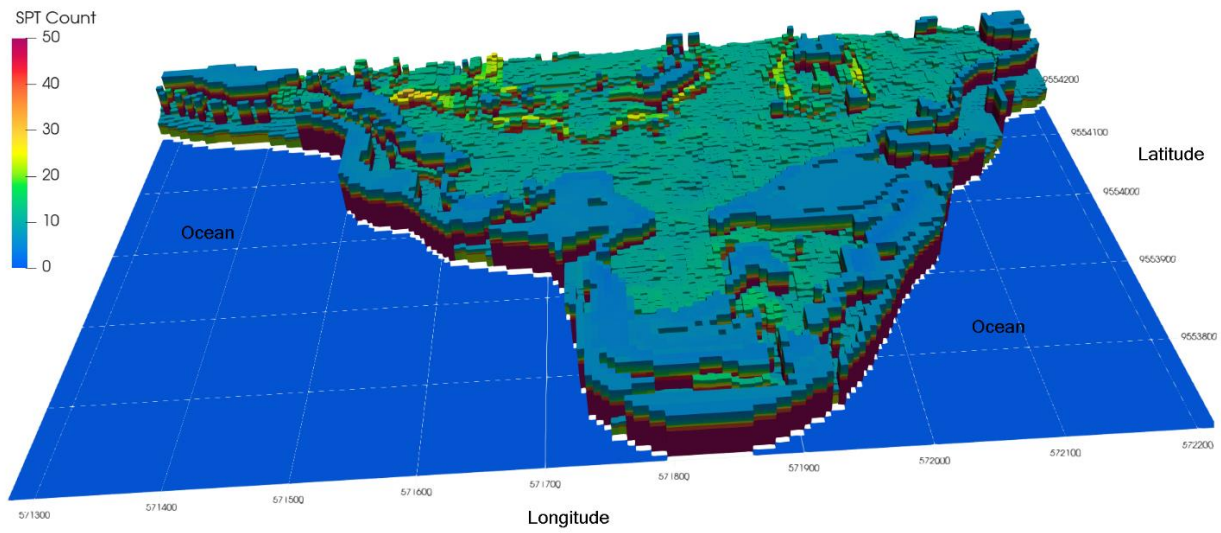


Figure 3: 3D model of relative subsurface strength of project site

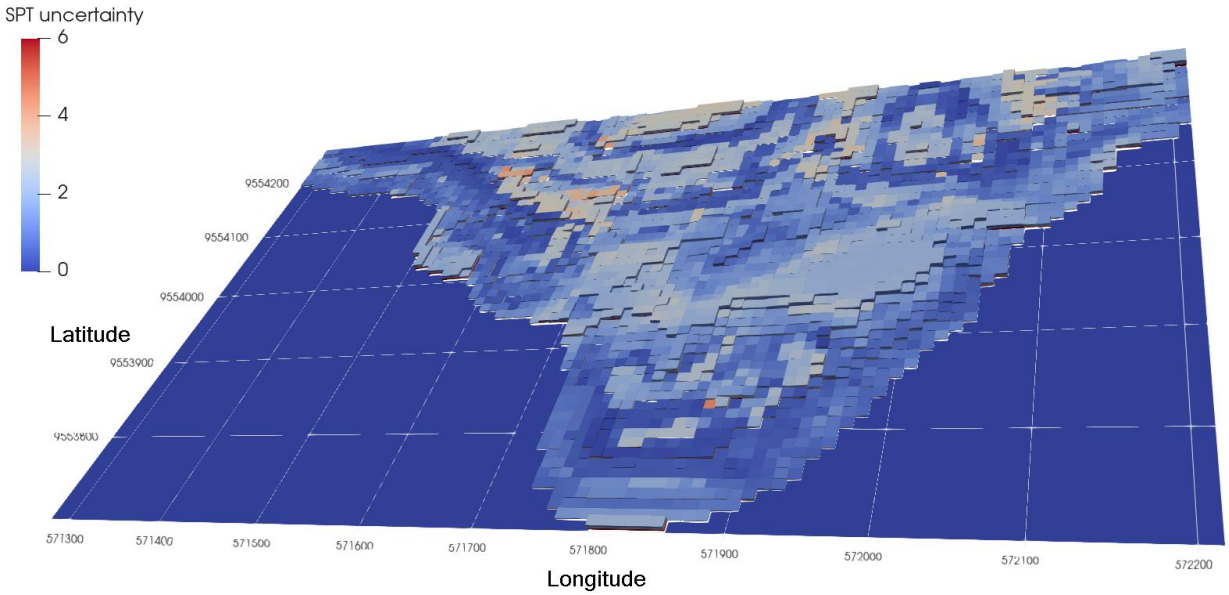


Figure 4: Prediction width at 95% confidence interval for 3D SPT count

## 5. Conclusions

3D model representation is very important in enhancing geotechnical investigations and improving site characterization. It has been widely used in geologic investigations but not so popular with geotechnical investigations. This study reviewed progress of 3D modelling in geotechnical investigations including current practices and opportunities for improvement. It showed that there has been an increasing demand for 3D representation of geotechnical investigations, which pushed the growth in adoption of 3D modelling

techniques. The new techniques also complement the traditional investigation techniques. An indication of the growth in 3D modelling in geotechnical engineering is seen in the number of dedicated software that have since been developed. However, most dedicated software lack some important functionalities such as uncertainty assessment. Recent use of computer scripts as add-on to main software have seen improved versatility in incorporating uncertainty assessment in 3D models. They have a huge potential in opening up wide application of 3D modelling in geotechnical engineering.

Three broad application areas for 3D modelling in geotechnical investigations are subsurface risk assessment, 3D visualization, and identification of important subsurface sections/points. A case study application of 3D modelling was shown to summarize on-going activities in the literature.

**Acknowledgements**

This study reported software developed by different companies. The companies are acknowledged. Example case study data was collected by different companies involved in geotechnical investigations of proposed site for construction of inland container depot in Mombasa. The staff involved are highly acknowledged.

**Statements and Declarations**

No funding was received to assist with the preparation of this manuscript. The authors have no competing interests to declare that are relevant to the content of this article.

**Data availability**

The datasets generated during the current study are available from the corresponding author on reasonable request.

## REFERENCES

Aghamolaie, I., Lashkaripour, G.R., Ghafoori, M., Hafezi Moghaddas, N., 2019. 3D geotechnical modeling of subsurface soils in Kerman city, southeast Iran. Bull. Eng. Geol. Environ. 78, 1385–1400. https://doi.org/10.1007/s10064-018-1240-7

Ahmed, C., Mohammed, A., Tahir, A., 2020. Geostatistics of strength, modeling and GIS mapping of soil properties for residential purpose for Sulaimani City soils, Kurdistan Region, Iraq. Model. Earth Syst. Environ. 6, 879–893. https://doi.org/10.1007/s40808-020-00715-y

Akiska, S., 2013. 3D Subsurface Modeling of Mineralization: A Case Study from Handeresi (Çanakkale, NW Turkey) Pb-Zn-Cu Deposit. Turk. J. EARTH Sci. https://doi.org/10.3906/yer-1206-1

Aldefae, A.H., Mohammed, J., Saleem, H.D., 2020. Digital maps of mechanical geotechnical parameters using GIS. Cogent Eng. 7, 1779563. https://doi.org/10.1080/23311916.2020.1779563

Alqadad, A., Shahrour, I., Sukik, A., 2017. Smart system for safe and optimal soil investigation in urban areas. Undergr. Space 2, 220–226. https://doi.org/10.1016/j.undsp.2017.10.003

Arisona, A., Ishola, K.S., Nawawi, M.N.M., 2020. Subsurface void mapping using geophysical and geotechnical techniques with uncertainties estimation: case study of Kinta Valley, Perak, Malaysia. SN Appl. Sci. 2, 1171. https://doi.org/10.1007/s42452-020-2967-x

Auken, E., Boesen, T., Christiansen, A.V., 2017. A Review of Airborne Electromagnetic Methods With Focus on Geotechnical and Hydrological Applications From 2007 to 2017, in: Advances in Geophysics. Elsevier, pp. 47–93. https://doi.org/10.1016/bs.agph.2017.10.002

Awan, T.A., Arshid, M.U., Riaz, M.S., Houda, M., Abdallah, M., Shahkar, M., Aghdam, M.M., Azab, M., 2022. Sub-Surface Geotechnical Data Visualization of Inaccessible Sites Using GIS. ISPRS Int. J. Geo-Inf. 11, 368. https://doi.org/10.3390/ijgi11070368

Azrief Azahar, M., Farhan Zakiran Mahadi, N., Rusli, Q.N., Narendranathan, N., Lee, E.C., 2019. Use of geophysics for site investigations and earthworks assessments. IOP Conf. Ser. Mater. Sci. Eng. 512, 012007. https://doi.org/10.1088/1757-899X/512/1/012007

Bačić, M., Librić, L., Kaćunić, D.J., Kovačević, M.S., 2020. The Usefulness of Seismic Surveys for Geotechnical Engineering in Karst: Some Practical Examples. Geosciences 10, 406. https://doi.org/10.3390/geosciences10100406

Beygi, M., Keshavarz, A., Abbaspour, M., Vali, R., 2020. 3D numerical study of the piled raft behaviour due to groundwater level changes in the frictional soil. Int. J. Geotech. Eng. 14, 665–672. https://doi.org/10.1080/19386362.2019.1677326

Bo, M.W., 2022. Geotechnical ground investigation. World Scientific, Singapore ; Hackensack, NJ ; London.

Brady, P.V., Freeze, G.A., Kuhlman, K.L., Hardin, E.L., Sassani, D.C., MacKinnon, R.J., 2017. Deep borehole disposal of nuclear waste, in: Geological Repository Systems for Safe Disposal of Spent Nuclear Fuels and Radioactive Waste. Elsevier, pp. 89–112. https://doi.org/10.1016/B978-0-08-100642-9.00004-9

Bui, N., Merschbrock, C., Munkvold, B.E., 2016. A Review of Building Information Modelling for Construction in Developing Countries. Procedia Eng. 164, 487–494. https://doi.org/10.1016/j.proeng.2016.11.649

Bullejos, M., Cabezas, D., Martín-Martín, M., Alcalá, F.J., 2022. A Python Application for Visualizing the 3D Stratigraphic Architecture of the Onshore Llobregat River Delta in NE Spain. Water 14, 1882. https://doi.org/10.3390/w14121882

Caballero, S.R., Bheemasetti, T.V., Puppala, A.J., Chakraborty, S., 2022. Geotechnical Visualization and Three-Dimensional Geostatistics Modeling of Highly Variable Soils of a Hydraulic Fill Dam. J. Geotech. Geoenvironmental Eng. 148, 05022006. https://doi.org/10.1061/(ASCE)GT.1943-5606.0002872

Chandran, D., Anbazhagan, P., 2017. Subsurface profiling using integrated geophysical methods for 2D site response analysis in Bangalore city, India: a new approach. J. Geophys. Eng. 14, 1300–1314. https://doi.org/10.1088/1742-2140/aa7bc4

Chen, S.-E., Sumitro, P., Boyle, C., 2016. Remote sensing techniques for geo-problem applications. Jpn. Geotech. Soc. Spec. Publ. 2, 207–211. https://doi.org/10.3208/jgssp.TC302-05

Chimdesa, Firanboni Fituma, Chimdesa, Firaol Fituma, Jilo, N.Z., Hulagabali, A., Babalola, O.E., Tiyasha, T., Ramaswamy, K., Kumar, A., Bhagat, S.K., 2023. Numerical analysis of pile group, piled raft, and footing using finite element software PLAXIS 2D and GEO5. Sci. Rep. 13, 15875. https://doi.org/10.1038/s41598-023-42783-x

Cueto, M., Olona, J., Fernández-Viejo, G., Pando, L., López-Fernández, C., 2018. Karst-induced sinkhole detection using an integrated geophysical survey: a case study along the Riyadh Metro Line 3 (Saudi Arabia). Surf. Geophys. 16, 270–281. https://doi.org/10.3997/1873-0604.2018003

De La Varga, M., Schaaf, A., Wellmann, F., 2019. GemPy 1.0: open-source stochastic geological modeling and inversion. Geosci. Model Dev. 12, 1–32. https://doi.org/10.5194/gmd-12-1-2019

De Rienzo, F., Oreste, P., Pelizza, S., 2008. Subsurface geological-geotechnical modelling to sustain underground civil planning. Eng. Geol. 96, 187–204. https://doi.org/10.1016/j.enggeo.2007.11.002

Devi, A., Israil, M., Anbalagan, R., Gupta, P.K., 2017. Subsurface soil characterization using geoelectrical and geotechnical investigations at a bridge site in Uttarakhand Himalayan region. J. Appl. Geophys. 144, 78–85. https://doi.org/10.1016/j.jappgeo.2017.07.005

Dezert, T., Fargier, Y., Palma Lopes, S., Côte, P., 2019. Geophysical and geotechnical methods for fluvial levee investigation: A review. Eng. Geol. 260, 105206. https://doi.org/10.1016/j.enggeo.2019.105206

Dong, M., Neukum, C., Hu, H., Azzam, R., 2015. Real 3D geotechnical modeling in engineering geology: a case study from the inner city of Aachen, Germany. Bull. Eng. Geol. Environ. 74, 281–300. https://doi.org/10.1007/s10064-014-0640-6

Eastman, C.M., Teicholz, P.M., Sacks, R., Lee, G., 2018. BIM handbook: a guide to building information modeling for owners, managers, designers, engineers and contractors, Third edition. ed. Wiley, Hoboken, New Jersey.

El Sibaii, M., Granja, J., Bidarra, L., Azenha, M., 2022. Towards efficient BIM use of geotechnical data from geotechnical investigations. J. Inf. Technol. Constr. 27, 393–415. https://doi.org/10.36680/j.itcon.2022.019

El-Banna, M.A., Basha, A.M., Beshr, A.A.A., 2023. Creating digital maps for geotechnical characteristics of soil based on GIS technology and remote sensing. Open Geosci. 15, 20220495. https://doi.org/10.1515/geo-2022-0495

Elsheikh, A.H., Elsheikh, M., 2014. A reliable triangular mesh intersection algorithm and its application in geological modelling. Eng. Comput. 30, 143–157. https://doi.org/10.1007/s00366-012-0297-3

Frank, T., Tertois, A.-L., Mallet, J.-L., 2007. 3D-reconstruction of complex geological interfaces from irregularly distributed and noisy point data. Comput. Geosci. 33, 932–943. https://doi.org/10.1016/j.cageo.2006.11.014

Griffiths, J.S., 2014. Feet on the ground: engineering geology past, present and future. Q. J. Eng. Geol. Hydrogeol. 47, 116–143. https://doi.org/10.1144/qjegh2013-087

Guan, Z., Wang, Y., 2021. Rational determination of cone penetration test quantity in a two-dimensional vertical cross-section for site investigation. Tunn. Undergr. Space Technol. 109, 103771. https://doi.org/10.1016/j.tust.2020.103771

Guo, J., Wang, X., Wang, J., Dai, X., Wu, L., Li, C., Li, F., Liu, S., Jessell, M.W., 2021. Three-dimensional geological modeling and spatial analysis from geotechnical borehole data using an implicit surface and marching tetrahedra algorithm. Eng. Geol. 284, 106047. https://doi.org/10.1016/j.enggeo.2021.106047

Hack, R., Orlic, B., Ozmutlu, S., Zhu, S., Rengers, N., 2006. Three and more dimensional modelling in geo-engineering. Bull. Eng. Geol. Environ. 65, 143–153. https://doi.org/10.1007/s10064-005-0021-2

Hamman, E., du Plooy, D., Seery, J., 2017. Data management and geotechnical models, in: Wesseloo, J., Wesseloo, J. (Eds.), . Presented at the Deep Mining 2017: Eighth International Conference on Deep and High Stress Mining, Australian Centre for Geomechanics, Perth, pp. 461–487.

He, H., Xiao, J., He, J., Wei, B., Ma, X., Huang, F., Cai, X., Zhou, Y., Bi, J., Zhao, Y., Wang, C., Wei, J., 2023. Three-Dimensional Geological Modeling of the Shallow Subsurface and Its Application: A Case Study in Tongzhou District, Beijing, China. Appl. Sci. 13, 1932. https://doi.org/10.3390/app13031932

Hemeda, S., 2019. 3D finite element coupled analysis model for geotechnical and complex structural problems of historic masonry structures: conservation of Abu Serga church, Cairo, Egypt. Herit. Sci. 7, 6. https://doi.org/10.1186/s40494-019-0248-z

Hool, G.A., Kinne, W.S., 1923. Foundations, Abutments, and Footings. McGraw-Hill.

Hunt, R.E., 2007. Geotechnical investigation methods: a field guide for geotechnical engineers. CRC/Taylor & Francis, Boca Raton, FL.

Kahlström, M., Mortensen, P.-A., Hauser, C., Hansen Børner, N., 2021. Use of a 3D stratigraphic model as tool for improved communication and risk assessment in large infrastructure projects. IOP Conf. Ser. Earth Environ. Sci. 710, 012038. https://doi.org/10.1088/1755-1315/710/1/012038

Kaufmann, O., Martin, T., 2008. 3D geological modelling from boreholes, cross-sections and geological maps, application over former natural gas storages in coal mines. Comput. Geosci. 34, 278–290. https://doi.org/10.1016/j.cageo.2007.09.005

Kim, M., Kim, H.-S., Chung, C.-K., 2020. A Three-Dimensional Geotechnical Spatial Modeling Method for Borehole Dataset Using Optimization of Geostatistical Approaches. KSCE J. Civ. Eng. 24, 778–793. https://doi.org/10.1007/s12205-020-1379-1

Labib, M., Nashed, A., 2013. GIS and geotechnical mapping of expansive soil in Toshka region. Ain Shams Eng. J. 4, 423–433. https://doi.org/10.1016/j.asej.2012.11.005

Lee, F., Tan, T., Karunaratne, G.P., Lee, S., 1990. Geotechnical Data Management System. J. Comput. Civ. Eng. 4, 239–254. https://doi.org/10.1061/(ASCE)0887-3801(1990)4:3(239)

Lemon, A.M., Jones, N.L., 2003. Building solid models from boreholes and user-defined cross-sections. Comput. Geosci. 29, 547–555. https://doi.org/10.1016/S0098-3004(03)00051-7

Liu, D., He, L., Wu, Q., Gao, Y., Liu, B., Liu, S., Luo, H., 2021. Construction and application of the 3D geo-hazard monitoring and early warning platform. Open Geosci. 13, 1040–1052. https://doi.org/10.1515/geo-2020-0293

Liu, X., Dong, X., Leskovar, D.I., 2016. Ground penetrating radar for underground sensing in agriculture: a review. Int. Agrophysics 30, 533–543. https://doi.org/10.1515/intag-2016-0010

Liu, Y., Ng, Y.C.H., Zhang, Y., Yang, P., Ku, T., 2023. Incorporating geotechnical and geophysical investigations for underground obstruction detection: A case study. Undergr. Space 11, 116–129. https://doi.org/10.1016/j.undsp.2022.12.003

Longoni, L., Arosio, D., Scaioni, M., Papini, M., Zanzi, L., Roncella, R., Brambilla, D., 2012. Surface and subsurface non-invasive investigations to improve the characterization of a fractured rock mass. J. Geophys. Eng. 9, 461–472. https://doi.org/10.1088/1742-2132/9/5/461

Look, B.G., 2007. Handbook of Geotechnical Investigation and Design Tables, 0 ed. Taylor & Francis. https://doi.org/10.1201/9780203946602

Mallet, J.L., 1997. Discrete modeling for natural objects. Math. Geol. 29, 199–219. https://doi.org/10.1007/BF02769628

Marache, A., Dubost, J., Breysse, D., Denis, A., Dominique, S., 2009. Understanding subsurface geological and geotechnical complexity at various scales in urban soils using a 3D

model. Georisk Assess. Manag. Risk Eng. Syst. Geohazards 3, 192–205. https://doi.org/10.1080/17499510802711994

Masoud, A.A., Saad, A.M., El Shafaey, O.N.H., 2022. Geotechnical database building and 3D modeling of the soil in Medina, Saudi Arabia. Arab. J. Geosci. 15, 506. https://doi.org/10.1007/s12517-022-09781-1

McNally, G.H., 1990. The Prediction of Geotechnical Rock Properties from Sonic and Neutron Logs. Explor. Geophys. 21, 65–71. https://doi.org/10.1071/EG990065

Medhus, A.B., Klinkby, L. (Eds.), 2023. Engineering geophysics. CRC Press, Taylor & Francis Group, Boca Raton.

Mei, G., 2014. Summary on Several Key Techniques in 3D Geological Modeling. Sci. World J. 2014, 1–11. https://doi.org/10.1155/2014/723832

Mielby, S., Sandersen, P.B.E., 2017. Development of a 3D geological/hydrogeological model targeted at sustainable management of the urban water cycle in Odense City, Denmark. Procedia Eng. 209, 75–82. https://doi.org/10.1016/j.proeng.2017.11.132

Montanari, F., Previatello, P., 1979. Automatic geotechnical data management. Bull. Int. Assoc. Eng. Geol. 19, 311–314. https://doi.org/10.1007/BF02600494

Moore, R.R., Johnson, S.E., 2001. Three-dimensional reconstruction and modelling of complexly folded surfaces using Mathematica. Comput. Geosci. 27, 401–418. https://doi.org/10.1016/S0098-3004(00)00079-0

Optum Computational Engineering, 2020. Optum G3: Geotechnical design software.

Orhan, A., Tosun, H., 2010. Visualization of geotechnical data by means of geographic information system: a case study in Eskisehir city (NW Turkey). Environ. Earth Sci. 61, 455–465. https://doi.org/10.1007/s12665-009-0357-1

Orlić, B., 1997. Predicting subsurface conditions for geotechnical modelling, ITC publication. International Institute for Aerospace Survey and Earth Sciences, Delft.

Otake, Y., Honjo, Y., 2022. Challenges in geotechnical design revealed by reliability assessment: Review and future perspectives. Soils Found. 62, 101129. https://doi.org/10.1016/j.sandf.2022.101129

Ozmutlu, S., Hack, R., 2006. 3D modelling system for ground engineering, in: Rosenbaum, M.S., Turner, A.K. (Eds.), New Paradigms in Subsurface Prediction, Lecture Notes in Earth Sciences. Springer Berlin Heidelberg, Berlin, Heidelberg, pp. 253–260. https://doi.org/10.1007/3-540-48019-6_22

Paillet, F., Saunders, W. (Eds.), 1990. Geophysical Applications for Geotechnical Investigations. ASTM International, 100 Barr Harbor Drive, PO Box C700, West Conshohocken, PA 19428-2959. https://doi.org/10.1520/STP1101-EB

Pellerin, L., 2002. Applications Of Electrical And Electromagnetic Methods For Environmental And Geotechnical Investigations. Surv. Geophys. 23, 101–132. https://doi.org/10.1023/A:1015044200567

Petrone, P., Allocca, V., Fusco, F., Incontri, P., De Vita, P., 2023. Engineering geological 3D modeling and geotechnical characterization in the framework of technical rules for geotechnical design: the case study of the Nola's logistic plant (southern Italy). Bull. Eng. Geol. Environ. 82, 12. https://doi.org/10.1007/s10064-022-03017-y

Pinheiro, M., Emery, X., Miranda, T., Lamas, L., Espada, M., 2018. Modelling Geotechnical Heterogeneities Using Geostatistical Simulation and Finite Differences Analysis. Minerals 8, 52. https://doi.org/10.3390/min8020052

Priya, D., Dodagoudar, G.R., 2017. Building 3D subsurface models and mapping depth to weathered rock in Chennai, south India. J. Geomat. 11, 191–200.

R Core team, 2023. R: A language and environment for statistical computing.

Rasmussen, L.L., 2020. U n B l o c k s g e n : A Python library for 3D rock mass generation and analysis. SoftwareX 12, 100577. https://doi.org/10.1016/j.softx.2020.100577

Reiffsteck, P., Benoît, J., Bourdeau, C., Desanneaux, G., 2018. Enhancing Geotechnical Investigations Using Drilling Parameters. J. Geotech. Geoenvironmental Eng. 144, 04018006. https://doi.org/10.1061/(ASCE)GT.1943-5606.0001836

Rockware, 2023. RockWorks.

Romero-Ruiz, A., Linde, N., Keller, T., Or, D., 2018. A Review of Geophysical Methods for Soil Structure Characterization. Rev. Geophys. 56, 672–697. https://doi.org/10.1029/2018RG000611

Satyanaga, A., Aventian, G.D., Makenova, Y., Zhakiyeva, A., Kamaliyeva, Z., Moon, S.-W., Kim, J., 2023. Building Information Modelling for Application in Geotechnical Engineering. Infrastructures 8, 103. https://doi.org/10.3390/infrastructures8060103

Schorpp, L., Straubhaar, J., Renard, P., 2022. Automated Hierarchical 3D Modeling of Quaternary Aquifers: The ArchPy Approach. Front. Earth Sci. 10, 884075. https://doi.org/10.3389/feart.2022.884075

Seequent, 2021. Leapfrog Works: Building a 3D geological model.

Sergay, G., 2023. WLD 3D Visualizer.

Siggins, A.F., 1990. Ground Penetrating Radar in Geotechnical Applications. Explor. Geophys. 21, 175–186. https://doi.org/10.1071/EG990175

SoilVision, 2012. SVSolid.

Soupios, P.M., Georgakopoulos, P., Papadopoulos, N., Saltas, V., Andreadakis, A., Vallianatos, F., Sarris, A., Makris, J.P., 2007. Use of engineering geophysics to investigate a site for a building foundation. J. Geophys. Eng. 4, 94–103. https://doi.org/10.1088/1742-2132/4/1/011

Sulistijo, B., Anwar, A.S.K., 2013. Integrated Site Investigation Method to Analyze Subsurface Condition for the Belt Conveyor. Procedia Earth Planet. Sci. 6, 369–376. https://doi.org/10.1016/j.proeps.2013.01.048

Toll, D.G., Barr, R.J., 2001. A decision support system for geotechnical applications. Comput. Geotech. 28, 575–590. https://doi.org/10.1016/S0266-352X(01)00014-3

Touch, S., Likitlersuang, S., Pipatpongsa, T., 2014. 3D geological modelling and geotechnical characteristics of Phnom Penh subsoils in Cambodia. Eng. Geol. 178, 58–69. https://doi.org/10.1016/j.enggeo.2014.06.010

Tsai, C.-C., Lin, C.-H., 2022. Review and Future Perspective of Geophysical Methods Applied in Nearshore Site Characterization. J. Mar. Sci. Eng. 10, 344. https://doi.org/10.3390/jmse10030344

Valeria, N., Roberta, V., Vittoria, C., Domenico, A., Filomena, de S., Stefania, F., 2019. A new frontier of BIM process: Geotechnical BIM. Proc. XVII Eur. Conf. Soil Mech. Geotech. Eng. 3356–3362. https://doi.org/10.32075/17ECSMGE-2019-0682

Vanneschi, C., Salvini, R., Massa, G., Riccucci, S., Borsani, A., 2014. Geological 3D modeling for excavation activity in an underground marble quarry in the Apuan Alps (Italy). Comput. Geosci. 69, 41–54. https://doi.org/10.1016/j.cageo.2014.04.009

Venmans, A., Schokker, J., Dambrink, R., Maljes, D., Heerema, J., 2015. Mapping Geotechnical Risks for Infrastructural Works in Deltaic Areas, in: Geotechnical Safety and Risk V. IOS Press, Netherlands, pp. 886–889.

Von Hebel, C., Rudolph, S., Mester, A., Huisman, J.A., Kumbhar, P., Vereecken, H., Van Der Kruk, J., 2014. Three-dimensional imaging of subsurface structural patterns using quantitative large-scale multiconfiguration electromagnetic induction data. Water Resour. Res. 50, 2732–2748. https://doi.org/10.1002/2013WR014864

Wang, Y., Shi, C., Li, X., 2022. Machine learning of geological details from borehole logs for development of high-resolution subsurface geological cross-section and geotechnical analysis. Georisk Assess. Manag. Risk Eng. Syst. Geohazards 16, 2–20. https://doi.org/10.1080/17499518.2021.1971254

Wu, S., Zhang, J.-M., Wang, R., 2021. Machine learning method for CPTu based 3D stratification of New Zealand geotechnical database sites. Adv. Eng. Inform. 50, 101397. https://doi.org/10.1016/j.aei.2021.101397

Wu, X., Liu, G., Weng, Z., Tian, Y., Zhang, Z., Li, Y., Chen, G., 2021. Constructing 3D geological models based on large-scale geological maps. Open Geosci. 13, 851–866. https://doi.org/10.1515/geo-2020-0270

Zhang, Z., 2011. Achievements and problems of geotechnical engineering investigation in China. J. Zhejiang Univ.-Sci. A 12, 87–102. https://doi.org/10.1631/jzus.A1000433

# Techno-Economic Analysis of Hybrid Solar-Diesel Minigrids in Kenya: A Case Study of the Retrofitting Eldas Diesel Minigrid - Pilot Site

L. K. Kamanja*, K. Wachira, D. G. Nyandera, E. Chebet, K, Mukangula. F. K. Koome, S. Waita

Kenya Power and Lighting Company P.O Box 30099- 00100 Nairobi

* lilkany06@gmail.com

**Abstract**

Generation of electricity from fossil fuels globally has led to the emission of greenhouse gases, which has been a major contributor of global warming. In addition, one of the biggest challenges in the developing world is the provision of reliable and affordable electricity access to remote and marginalized people where grid extension is too expensive.

Off-grid electrification program in Kenya for remote centres has been running since the early 80's. Until very recently, all sites were 100% powered by diesel generators. The Ministry of Energy is supporting the Rural Electrification and Renewable Energy Corporation and Kenya Power & Lighting Co. Ltd to hybridize 18 sites to maximize the use of renewable energy, reduce fuel costs and lower carbon emissions.

The government of Kenya spends up to 5 billion Ksh annually on diesel fuel for generators powering the remote sites namely (Mandera, Wajir, Kakuma, Merti, Habaswein, Elwak, Baragoi, Mfangano, Rhamu, Eldas, Takaba, Lokichoggio, Lokori, Laisamis, Faza, Kiunga, Hulugho, North Horr, Lokitaung, Dadaab, Maikona Lokiriama, Banisa).

A techno-economic analysis of retrofitting Eldas site shows that a 315.6 kW hybrid solar PV diesel hybrid system with four generators (2*65 kVA, 2*135 kVA) is sufficient to power the town of Eldas and its surroundings. Financial analysis shows that the payback period after retrofitting the minigrid is 9.5 years. In addition, 3,284 tons of Carbon Dioxide is saved. Hybridizing all the sites shows that the government of Kenya will save up to 3 billion Kenya Shillings per year.

**Key words:** Solar PV-Diesel Minigrid, Payback Period, Greenhouse Gas Emissions,Techno-economic analysis, Eldas

## 1. Introduction

Over the years diesel generators in Kenya have been used to power households in off-grid rural setups and towns where the extension of the grid is prohibitively expensive. The use of diesel generators has been preferred due to their capability to supply power for 24 hours. However, the increased fuel prices and harmful carbon emissions have made the use of diesel generators only unattractive and expensive. Renewable energy systems on the other hand have been adapted due to the concerns of greenhouse gas emissions, which are contributing to climate change (Yamegueu et al. 2011).

The use of hybrid systems (diesel and solar and storage) is gaining popularity, because the use of solar energy is maximized during the day, the stored energy in batteries is maximized during the night and optimal-sized diesel generators are used to supply extra power that may be required during the peak and night hours hence ensuring reliable power. In addition, other benefits accrued include; adoption of renewable energy systems, reduction of fuel costs and reduction of carbon footprint.

To this effect, the Ministry of Energy in Kenya is supporting the Rural Electrification and Renewable Energy Corporation and Kenya Power & Lighting Co. Ltd to hybridize 18 sites. The ministry of energy spends about Ksh. 62.7 million on diesel fuel costs for Eldas power station and Ksh. 5 billion for all the 23 diesel powered mini grids in off grid areas on annual basis. In this paper, we focus on doing a techno-economic analysis of hybridizing the diesel minigrid site in Eldas, Wajir County.

Numerous authors have conducted techno-economic analysis in various parts of the (Asrari et al. 2012; Himri et al. 2008; Nema et al. 2009; Rehman and Al-Hadhrami 2010; Said and Ahmed 2014; Yamegueu et al. 2011), however, we have not come across any published work for Kenya on techno-economic analysis of hybridizing the diesel minigrid site in Eldas.

## 2. Methodology

### 1.1 The existing layout of Eldas hybrid minigrid

Eldas' power plant currently consists of one diesel generator operational since 2016, a 1*300kVA diesel generator, one 36kWp Solar PV power plant installed in August 2015 and one step-up transformer 1MVA 415V/33kV. The solar plant has not been operational for 2 years.

### 1.2 Solar radiation analysis from satellite data

The Global horizontal irradiance (GHI) and temperature for the Eldas area ranges from 5 kWh/m$^2$ to 6.3 kWh/m$^2$. Temperature ranges from 26.6 $^0$C to 30.3 $^0$C.

### 1.3 The daily energy demand profile

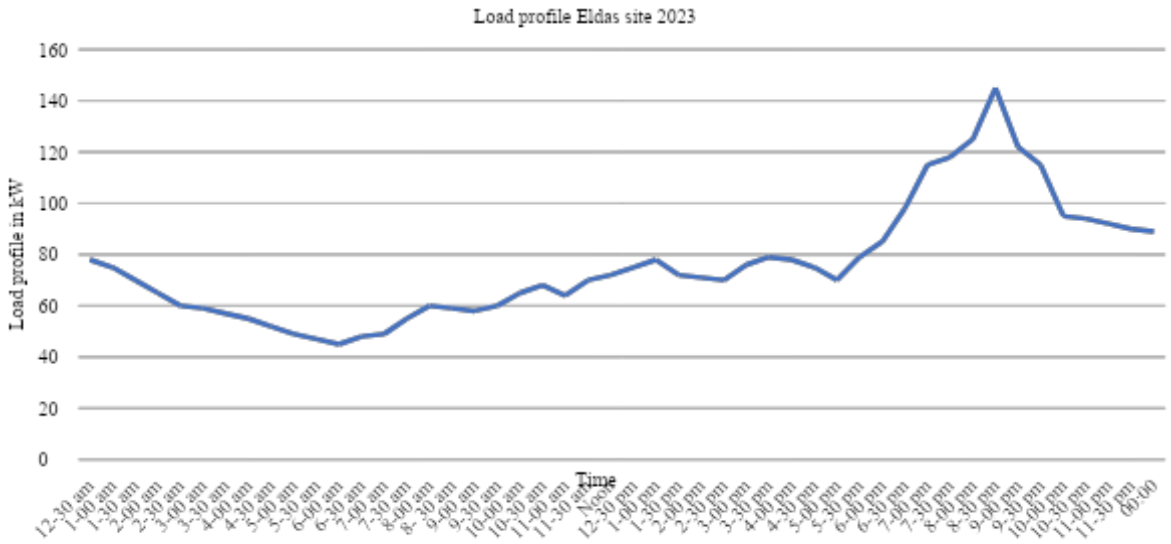


Fig 1: Daily energy demand profile at Eldas

The daily energy demand varies from a minimum of 45 kW during the day to a peak load of 145 kW at night as shown in Figure 1.

### 1.4 Hybrid minigrid sizing and simulation

Design and sizing was carried out as detailed below and verified by simulation using Homer software as shown in Table 1 and 2.

Table 1: Solar PV plant sizing

| Peak load | 2% yearly load increase in Zero year | 6.5% yearly load increase | 5% yearly load increase | 22% (Losses factor) |
|---|---|---|---|---|
| 145 kW | 147.9 kW | 202.6 kW | 259 kW | 315.5 kW |

Table 2: Generator sizing

| Peak load | 2% yearly load increase in Zero year | 6.5% yearly load increase | 5% yearly load increase | 30% (Losses) | 1/6 | 1/6 | 1/3 | 1/3 |
|---|---|---|---|---|---|---|---|---|
| 145 | 147.9 | 202.6358175 | 259 | 336.2 | 56.03 | 56.0 | 112.1 | 112.1 |

The distribution of the nominal power of the diesel generators is calculated as follows (33%/33%/16.7%/16.7%) as shown in Equations 1 and 2; to allow for the flexibility of picking load step-wise as it increases. Therefore, power per genset (at prime power)

$$\frac{Pnorm}{6} = \frac{336}{6} = 56 \text{ kVA} \quad \text{with a +/- 20\% margin} \qquad (1)$$

$$\frac{Pnorm}{3} = \frac{336}{3} = 112\text{kVA with a +/- 20\% margin.} \qquad (2)$$

Thus, the total kVA prime rating is 400 kVA with the sizes are; generator 1 – 65kVA, generator 2 – 65kVA, generator 3 – 135kVA, and generator 4 – 135kVA

Table 3: Battery capacity calculation

| Total daily energy kWh | Days of Autonomy | Battery efficiency | Depth of discharge | Battery capacity kWh |
|---|---|---|---|---|
| 476 | 1 | 0.95 | 0.8 | 626.3 |

Table 3 shows the parameters used to calculate the battery capacity using the formula in Equation 3

$$\frac{Total\ daily\ energy\ demand * Days\ of\ Autonomy}{Battery\ efficiency * Depth\ of\ Discharge} = 626\ kWh \qquad (3)$$

Thus battery-rated capacity 260 Ah, Nominal voltage 44.8V, and energy 12.544 kWh was selected.

### 1.5 PV module, inverter, converter capacity calculation and selection

The PV panel selected is monocrystalline 540W and the parameters for the module at standard test conditions include; Open–circuit voltage (Voc) 49.6 V, Short-circuit current (Isc) 13.86 V, Operating voltage (Vmpp) 41.64 V and Operating current (Impp) 12.97 V. The DC-DC converters (model PDS1-400K) selected are modular in design and housed inside a cabinet that can hold up to 8 pieces of the modular converters. Each modular converter is rated at 50kW with an input current of (0-130 A) and an input voltage of (250-800V). The cabinet is rated at 400kW. Therefore, the sizing of the PV array is as shown in Equation 4.

$$\text{No of panels} = \frac{315{,}900\ W}{540\ W} = 585 \text{ pcs} \qquad (4)$$

The voltage and current of the PV string should be within limits of the 50 kW converter input current and voltage levels. One string comprises 15 panels with a Voc of 744 V as shown in Equation 5, while Equation 6 shows the Voc with a temperature correction factor of 1.02

$$V_{oc} = 49.6\ V \times \text{No. Of panels per string (15)} = 744V_{oc} \qquad (5)$$

$$744V \times 1.02 = 758.88\ V_{oc} \qquad (6)$$

585 panels/15 panels per string = 39 strings

The string current ($I_{sc}$) is 13.86A and the number of strings per DC-DC combiner in use is 6. The maximum string array current per DC – DC combiner will therefore be:

$$=13.86A \times 6 = 83.16A \quad (7)$$

Peak power per converter =15 panels x 6 strings x 540W = 48,600W (8)

39 strings/6 strings per converter = 6.5=7 converters of 50kW each (9)

### 1.6 Battery Inverter sizing

The loads supplied are AC in nature thus there is a need to use a battery inverter for converting DC output to alternating current (AC) therefore; six inverters of 62.5 kVA were selected for this hybrid plant. The cabinet holding 8 pieces of inverters is rated at 500kVA. The inverter is selected in such a way as to achieve an AC-to-DC ratio of 1.1 to 1.25.

$$= 6 \times 62.5 = 375 \text{ Kva} \quad (10)$$

$$\text{DC/AC ratio} = \frac{375\ kW}{315.6\ W} = 1.18 \quad (11)$$

The selected inverter model PWS1-500KTL-NA specifications include a nominal power of 500 kVA, battery voltage range of (600-900V), DC current of 837 A, AC voltage of 400 V, and AC current of 720 A. In addition, two isolation transformers are also provided each rated at 200kVA.

### 1.7 The Eldas hybrid Minigrid schematic/single line diagram and homer simulation extract

**System Architecture**

| Component | Name | Size | Unit |
|---|---|---|---|
| **Generator #1** | GEN 1. 65 KVA / 52 kW | 52.0 | kW |
| **Generator #2** | GenGEN 2. 65 KVA / 52 kW | 52.0 | kW |
| **Generator #3** | GEN 3. 135 KVA / 108kW | 108 | kW |
| **Generator #4** | GEN 4. 135 KVA / 108kW (1) | 108 | kW |
| **PV** | Generic flat plate PV | 316 | kW |
| **Storage** | Generic 1kWh Li-Ion | 640 | strings |
| **System converter** | System Converter | 375 | kW |
| **Dispatch strategy** | HOMER Load Following | | |

Fig 2: Homer simulation extract

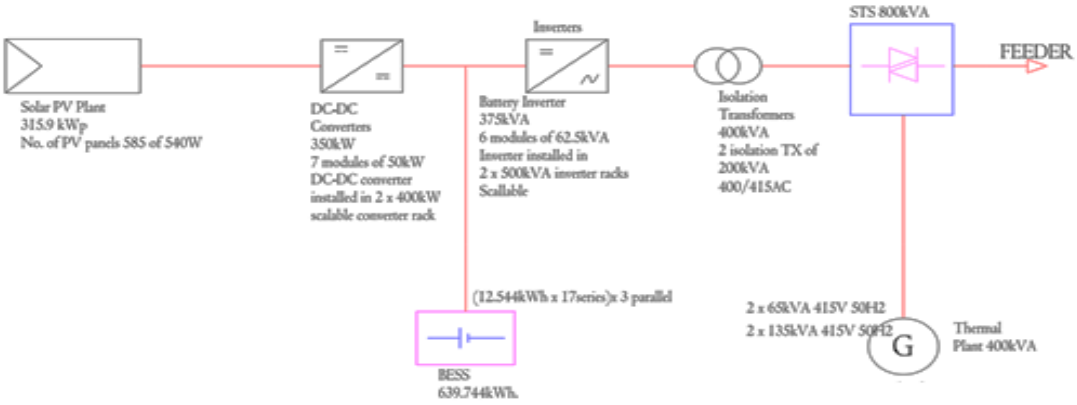


Fig 3:Eldas single line diagram

Figures 2 and 3 show the Homer simulation and Eldas single line diagram respectively

### 1.8 Economic feasibility to appraise the viability of the project

The overall project cost for the Eldas site is Ksh. 374, 151,594.5. The benefit accrued from the plant installed is the avoided cost of fuel. Ksh. 374,151,594.5 is spent annually on fuel for diesel generators at the Eldas site. Simulation through Homer shows that after installation 62% of the plant power supplying the loads will be from renewable energy. Therefore, the payback period can be calculated as follows

$$\text{Payback period} = \frac{Capital\ cost\ in\ Ksh}{(Avoided\ fraction\ of\ fuel\ cost\ in\ Ksh\ on\ an\ annual\ basis)} \quad (12)$$

The total amount of money spent by the government on fuel for the 23 diesel-powered sites is Ksh. 5,273,180,524.20. Equation 13 shows the estimation of the fuel cost savings. With the installation of the solar PV diesel plant in all 23 diesel-powered sites, the fuel consumption will be reduced by 62%.

Annual fuel cost for all the diesel-powered plants in Ksh x Renewable energy fraction (13)

### 1.9 Carbon Balance calculation

The carbon balance is calculated using the energy yield of the PV installation for one year as computed by the PVsyst simulation, the system lifetime of 25 years, the grid LCE given in $gCO_2/kWh$ and PV system LCE, given in tonnes of $CO_2$ ( the total amount of $CO_2$ emissions caused by the operation and construction of the PV installation) as shown in Figure 4.

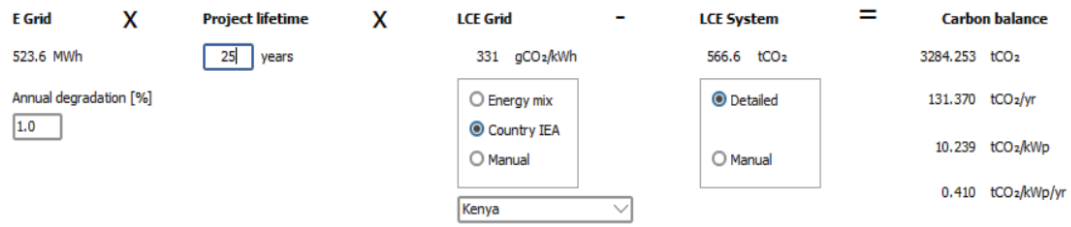


Fig 4: Carbon balance calculation

## 3. Results

Figure 5 shows an extract of the simulation from Homer. The total yearly production from solar PV is 511,712 kWh/yr, accounting for 62% of total generation. On the other hand, the annual generation from diesel generators is 317, 711 kWh/year which accounts for 38% of total generation.

**Production Summary**

| Component | Production (kWh/yr) | Percent |
|---|---|---|
| Generic flat plate PV | 511,712 | 61.7 |
| GEN 1. 65 KVA / 52 kW | 141,050 | 17.0 |
| GenGEN 2. 65 KVA / 52 kW | 103,223 | 12.4 |
| GEN 3. 135 KVA / 108kW | 73,429 | 8.85 |
| GEN 4. 135 KVA / 108kW (1) | 0 | 0 |
| Total | 829,414 | 100 |

Fig 5: Homer simulation extract

Economic analysis of hybridizing Eldas power plant shows that the payback period is 9.5 years as shown in equation 14. In addition, hybridizing all the sites shows that 3.3 billion shillings will be saved by the Kenan Government as shown in equation 15.

$$\text{Payback period} = (Ksh.\,374{,}151{,}594.5)/\ (62{,}745{,}216.00 * .62\ ) = 9.5 \text{ years} \quad (14)$$

$$\text{Ksh. } 5{,}273{,}180{,}524.20 \text{ x } 0.62 \text{ (renewable energy fraction)} = 3{,}269{,}371{,}925 \quad (15)$$

## 4. Discussion

Design and simulation of the solar PV plant using Homer shows that a 315.6Wp solar PV, 400 kVA diesel generator set (65, 65, 135, 135) kVA, battery storage of 640 kWh will be sufficient to provide reliable power for the town of Eldas (for current loads and future loads).

Economic analysis shows that the payback period of hybridizing the plant is 9.5 years which is favorable as it is less than the lifetime of the solar-diesel hybrid plant. Hybridizing all the sites shows that 3.3 billion shillings will be saved which the government can channel to more useful areas of need. In addition, a carbon balance of

3284 tons of $CO_2$ is achieved. Diversified sources of energy to constitute the hybrid plant will also ensure reliable power at all times for the residents of Eldas and its environs.

## 5. Conclusions

In this work, we carried out a techno-economic analysis of hybridizing the Eldas site. Design and sizing was carried out and verified using Homer software. Economic analysis was also done to determine the payback period of hybridizing the Eldas site and the carbon balance was calculated. Therefore, this work shows that 315.6Wp solar PV, 400 kVA diesel generator set (65, 65, 135, 135) kVA, battery storage of 640 kWh will be sufficient to provide reliable power for the town of Eldas (for current loads and future loads).

In addition, the payback of the project is 9.5 years. Hybridizing all the diesel-powered sites also shows that the government of Kenya will save 3.3 billion shillings annually. A carbon balance of 3284 tons of $CO_2$ is also realized. Thus, the techno-economic analysis of hybridizing Eldas site shows that it is technically and financially viable.

## Acknowledgment

We wish to thank Kenya Power and Lighting Company (KPLC) for the provision of data and facilitation of funds to finance the hybridization of the project.

**References**


1. Asrari, et al.. 2012. “Economic Evaluation of Hybrid Renewable Energy Systems for Rural Electrification in Iran - A Case Study.” *Renewable and Sustainable Energy Reviews* 16(5): 3123–30. http://dx.doi.org/10.1016/j.rser.2012.02.052.
2. Himri, et al. 2008. “Techno-Economical Study of Hybrid Power System for a Remote Village in Algeria.” *Energy* 33(7): 1128–36.
3. Nema, et al.2009. “A Current and Future State of Art Development of Hybrid Energy System Using Wind and PV-Solar: A Review.” *Renewable and Sustainable Energy Reviews* 13(8): 2096–2103.
4. Rehman, et. al. 2010. “Study of a Solar PV-Diesel-Battery Hybrid Power System for a Remotely Located Population near Rafha, Saudi Arabia.” *Energy* 35(12): 4986–95.
5. Said, et al.. 2014. “Hybrid System of the Existing Central Diesel with Photovoltaics, Technical and Economic Feasibility, Case of Talmine.” *3rd International Symposium on Environment-Friendly Energies and Applications, EFEA 2014*.
6. Yamegueu, et al.2011. “Experimental Study of Electricity Generation by Solar PV/Diesel Hybrid Systems without Battery Storage for off-Grid Areas.” Renewable Energy 36(6): 1780–87.

# Performance Evaluation of Hydraulic Ram Pumping Systems for Small Scale Farmers: A Case Study of West Pokot County, Kenya

J.K. Osome[1, 2*], J. R. Kosgei[1], E. C. Kipkorir[1], G. N. Nyandwaro[1] and J. I. Sempewo[3]

[1] Moi University, P.O. Box 3900-30100 Eldoret, Kenya

[2] Ministry of Water, Sanitation & Irrigation, P.O. Box 49720-00100 Nairobi, Kenya

[3] Department of Civil & Environmental Engineering, College of Engineering Design Art and Technology; Makerere University, P.O. Box 7062; Uganda

**Email:** corresponding-author-jkisiaosome@gmail.com

**Abstract**

Hydraulic ram pump (hydram) has been in existence for more than two centuries. However, these pumps have been on the verge of extinction since the invention of motorized pumps, which are more powerful and efficient. Unfortunately, motorized pumps are expensive to acquire, operate and maintain. Their contribution to climate change and environmental degradation has steered the need for an alternative pumping technology. Therefore, as the world's technology shifts to green energy, hydram pumps need to be re-invented. In the late twentieth century, studies on hydram pumps have been revived with the aim of making them more efficient and economically competitive. Small scale farmers in West Pokot County, Kenya, have embraced the hydram technology, but due to low technical capacity; installed low performing hydram that operated under low efficiencies of below 30%, with the majority having operational failure due to inadequate designs. Hence, this study investigated the design and operation of these pumps. Thereafter, designed and assembled a hydram pump, using locally available materials, to supply water for domestic and small-scale agricultural use. The optimum efficiency achieved by the pump was 54%, with an optimum delivery flow rate of about 13 L/min.

**Keywords:** Efficiency; Green energy; Hydram; Motorized pump; Operational failure; Optimum delivery flow rate.

## 1) Introduction

Water is a basic commodity essential for human, industrial, and agricultural development (Januddi et al, 2018). The need for water has been the key motivation that drives humankind to venture ways of ensuring ease access to it through various pumping mechanisms (Mishra et al., 2018). The first self-pumping machine (hydram) that did not

require external energy was invented in 1796 by the Montgolfier brothers (Mohammed, 2019). These pumps were modified and utilized until the late nineteenth century after the invention of oil and electric-driven pumps (motorized pumps). Recently, the need for sustainable technology and renewable energy, especially in developing countries, has revived the interest in hydram technology (Kherde, et al., 2020).

A hydraulic ram pump is a simple pump consisting of a pressure chamber, two main valves (impulse and delivery valves), and interconnecting pipes (Sheikh, et al., 2013). The pump, with its simplicity, does not require external energy, either mechanical or electrical, to pump water (Harith et al., 2017). It utilizes the energy of water falling from a higher head, drive head, to pump a portion of the same water to a higher head, delivery head (Veljko et al., 2003). The operation of hydraulic ram pumps depends on the water hammer phenomenon that results from the sudden closure of the impulse valve (Tacke, 1988). The water hammer effect generates waves that open the delivery valve and water is delivered to a higher head (Verspuy & Tijsseling, 1993, Than, et al., 2019) see figure 1. The operation of a hydram is intermittent due to the cyclic opening and closing of the waste and delivery valves (Januddi, et al., 2018). The closure of the waste valve creates a high-pressure rise in the drive pipe. An air chamber is required to transform the high intermittent pumped flows into a continuous stream of flow (Rajaonison & Rakotondramiarana, 2019). The air valves allow air into the hydram to replace the air absorbed by the water due to the high pressure and mixing in the air chamber. (Laxmi, et al., 2015).

The effect of climatic change and global warming has adversely affected the water supply for domestic and agricultural use. The small-scaled farmers who depend on rain-fed agricultural systems have incurred loss due to unreliable rainfall patterns (Ochieng et al., 2016). These farmers are unable to irrigate their farms due to their limited financial capabilities to acquire and operate the oil or electric powered pumping systems. The solution is to look for an alternative that is cheaper and more self-efficient, the hydraulic ram pumping system (Hussin, et al., 2017). Therefore, a more reliable and cost-effective system for irrigation during unfortunate events and also to act as a water supply is required. The most appropriate system will be hydraulic ram pumps.

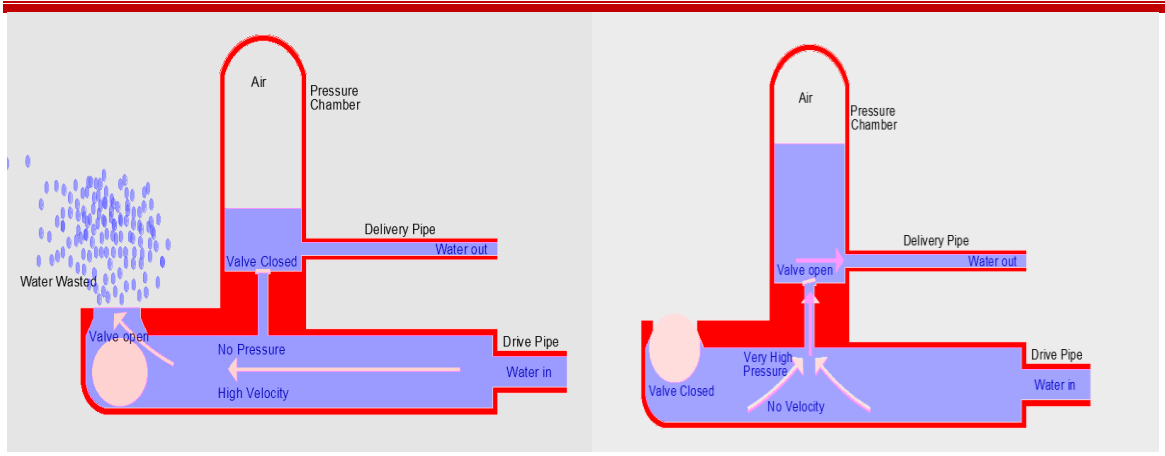


(a): Flow of water into the hydram (b) Flow of water after sudden closure of impulse valve

Figure 1: Operation of a hydram pump (Source: Januddi, et al., 2018)

The hydram pumping system is not a new technology in West Pokot County, Kenya. The farmers have embraced the technology because the area is endowed with a good river network system with good potential drive head for the pumping systems. The pumping systems in West Pokot are mainly used to supply water from the flowing rivers and streams for the purpose of domestic use and small-scale livestock farming. Unfortunately, the locals lack the technical know-how capacity of the hydram technology and therefore have fabricated and installed hydram pumps which were performing with low efficiencies. Therefore, this study investigated the existing hydraulic ram pumping systems in West Pokot County, Kenya, to assess these systems' design and performance characteristics. A low-cost hydram was designed and fabricated using locally available materials. The pump was tested by varying the drive and delivery head and its performance was assessed. The major limitation of the study was the behavior of the existing pumps for different drive and delivery heads where they were installed. Similarly, the designed pump was observed for a limited number of drive and delivery heads with assumption that the pump will simulate the actual site conditions.

## 2) Materials and Methods

### 2.1. Existing hydraulic ram pumping systems

The investigation was conducted on eight hydraulic ram pumping systems identified in West Pokot County, Kenya. These sites were chosen based on their availability and accessibility. Figure 2 shows the existing sites that were studied. These sites include; Karas, Kaibos, Chepkono, Kabichbich, Imonpoghet 1, Imonpoghet 2, Kamsis, and Kapsait. These systems were owned by individual members except the one found at

Chepkono area that was community owned system. These systems were used to supply water for domestic purpose and for small scale-livestock farming.

The evaluation focused on the design and performance criteria of the eight pump systems. On design criteria, the following components were assessed; materials used for the system, the size of pump and pipe components and the site conditions (stream flow rates, drive and delivery head). The performance criteria included; the efficiency of the system, failures and breakages. The existing pump were locally designed and fabricated by local artisans. The process of determining the design and performance criteria of the eight existing hydram systems were;

i. Direct interview and interrogation of the owners of the sites

ii. Observations and basic measurements

## 2.2. Construction and Experimentation of the hydram pump

The hydram pump was designed following Pawlick et al, (2018) and Watt, (1975) guidelines. Figure 3 shows a set-up of the hydram pump as done by Hussin, et al., (2017). The designed system was fabricated using PP-R pipes and fittings and GI fittings, as shown in Figure 4, since these materials are cheaply available and they have higher strength capacity to resist the pressures generated within the pump.

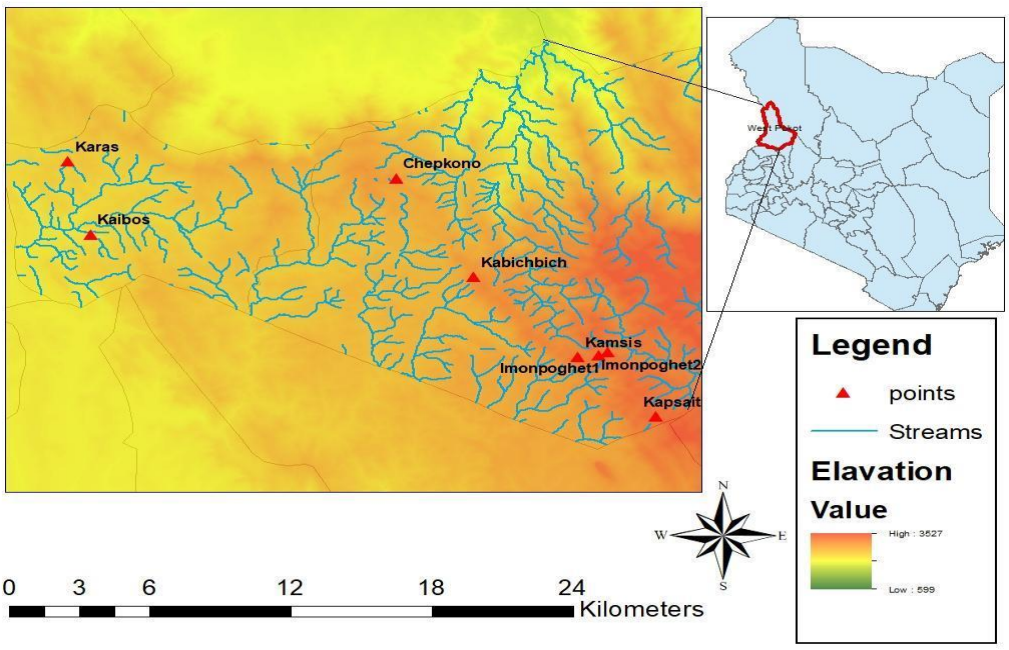


Figure 2: Location of the existing eight hydram pumping systems that were studied (Source: ArcGIS pro).

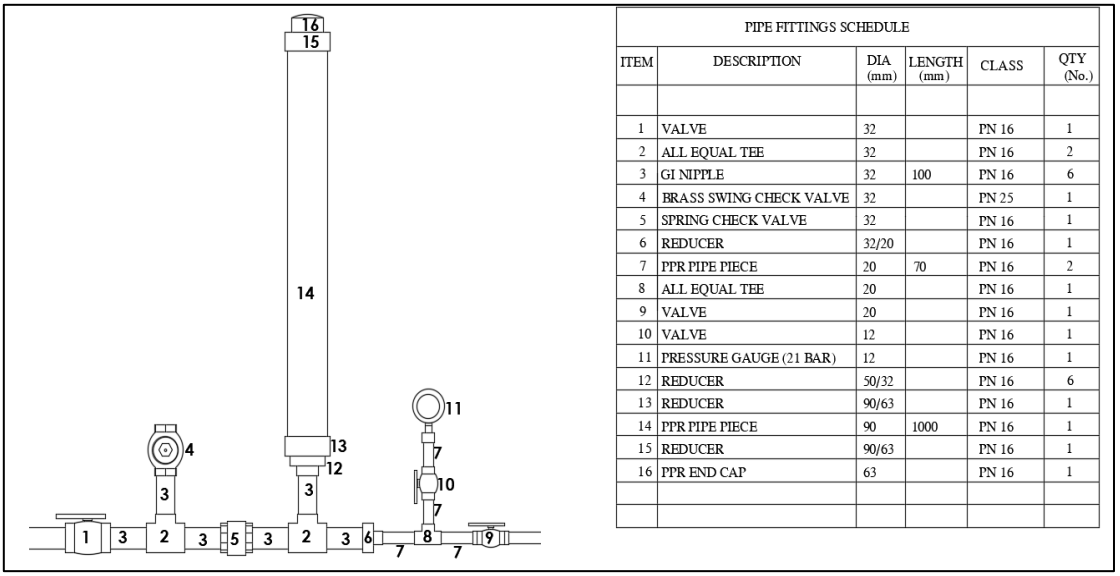


PIPE FITTINGS SCHEDULE

| ITEM | DESCRIPTION | DIA (mm) | LENGTH (mm) | CLASS | QTY (No.) |
|---|---|---|---|---|---|
| | | | | | |
| 1 | VALVE | 32 | | PN 16 | 1 |
| 2 | ALL EQUAL TEE | 32 | | PN 16 | 2 |
| 3 | GI NIPPLE | 32 | 100 | PN 16 | 6 |
| 4 | BRASS SWING CHECK VALVE | 32 | | PN 25 | 1 |
| 5 | SPRING CHECK VALVE | 32 | | PN 16 | 1 |
| 6 | REDUCER | 32/20 | | PN 16 | 1 |
| 7 | PPR PIPE PIECE | 20 | 70 | PN 16 | 2 |
| 8 | ALL EQUAL TEE | 20 | | PN 16 | 1 |
| 9 | VALVE | 20 | | PN 16 | 1 |
| 10 | VALVE | 12 | | PN 16 | 1 |
| 11 | PRESSURE GAUGE (21 BAR) | 12 | | PN 16 | 1 |
| 12 | REDUCER | 50/32 | | PN 16 | 6 |
| 13 | REDUCER | 90/63 | | PN 16 | 1 |
| 14 | PPR PIPE PIECE | 90 | 1000 | PN 16 | 1 |
| 15 | REDUCER | 90/63 | | PN 16 | 1 |
| 16 | PPR END CAP | 63 | | PN 16 | 1 |
| | | | | | |
| | | | | | |

Figure 3: Hydram schematic drawing for the designed hydram pump (Source: Mohammed, 2019).

(a) Components of the hydram (b) Complete assembled hydram pump

Figure 4: Fabrication of the Hydram pump (Source: Actual Site Photographs).

The drive head and the delivery head were the key parameters for investigation. The variation of both heads significantly affects the quantity of water delivered by the pump (Than, et al., 2019). Table 1 shows the drive heads and delivery heads used for the experimentation of the fabricated hydram.

Table 1: Experimental set-up parameters

| Experimentation | Drive head (m) | Delivery head (m) |
|---|---|---|
| 1 | 2.4 | 4.2 |
| 2 | 2.4 | 6.0 |

| | | |
|---|---|---|
| 3 | 2.8 | 10.0 |

## 3) Results

### Existing hydraulic ram pumping systems

The investigation of the existing eight hydram pumping system showed that 87.5% of hydram pumps are made up of steel. The majority of the pumps were of size 80/40mm configuration (that is, the inlet pipe size 80mm and outlet pipe size 40mm) and 80/25mm configuration (that is inlet pipe size 80mm and outlet pipe size 25mm) that constitute 50% and 37.5% respectively of the investigated pumps in West Pokot.

All sites had drive heads below 10m with delivery head above 40m and pressure chamber volume of greater than 2500 cm3, See figure 5.

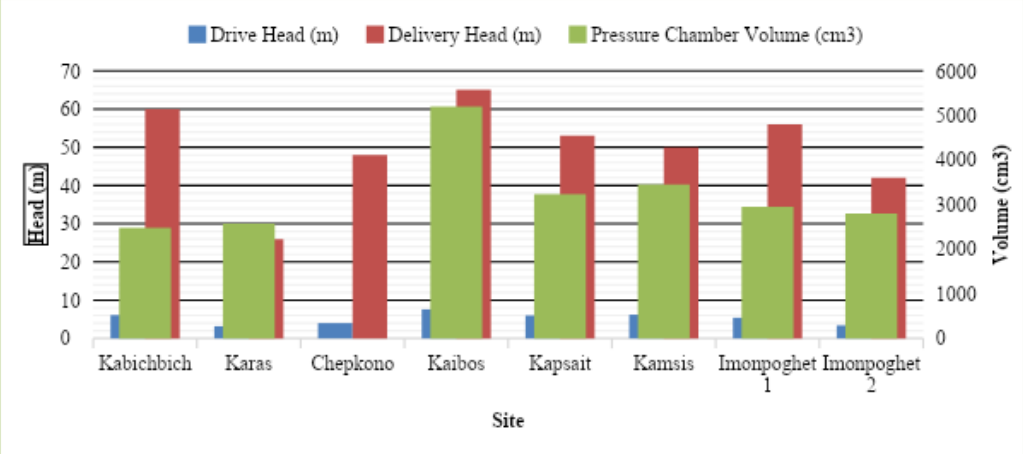


Figure 5: Relationship between drive head, delivery head and pressure chamber volume of existing eight hydram pumping systems.

These pumps had lower efficiencies of below 30% due to inadequate design of the system meaning, their designs are not tailor made to ensure pumps will be working as per site conditions (such as the drive head and the anticipated delivery heads) and pumping requirements that is the flow rates, build-up pressures and the water velocities within the pump as a results of site conditions.

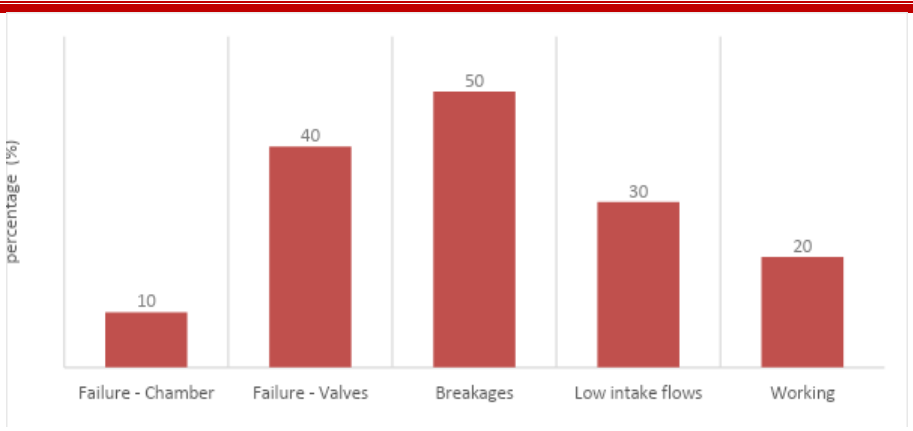


Figure 6: Performance evaluation of existing eight hydram pumps

The designed and fabricated hydram pump was able to obtain higher delivery flow rates, as shown in Figure 7. For the three experiments, a higher flow rate of 12.938 L/min was obtained on set-up 1 with a drive head of 2.4 m and a delivery head of 4.2 m. For a higher drive head of 2.8 m and delivery head of 10 m, a flow rate of 11.372 L/min was obtained.

The designed and fabricated hydram pump was able to obtain higher delivery flow rates, as shown in Figure 7. For the three experiments, a higher flow rate of 12.938 L/min was obtained on set-up 1 with a drive head of 2.4 m and a delivery head of 4.2 m. For a higher drive head of 2.8 m and delivery head of 10 m, a flow rate of 11.372 L/min was obtained.

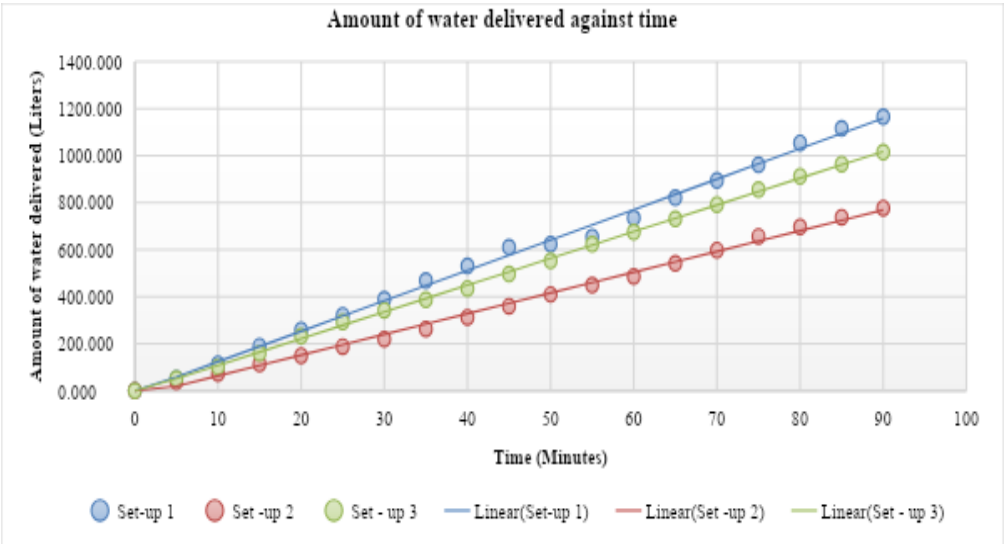


Figure 7: Amount of water delivered against time of the designed prototype hydram pump

The rate of the amount of water wasted by the pump was higher at higher heads as compared to the lower heads, see figure 8.

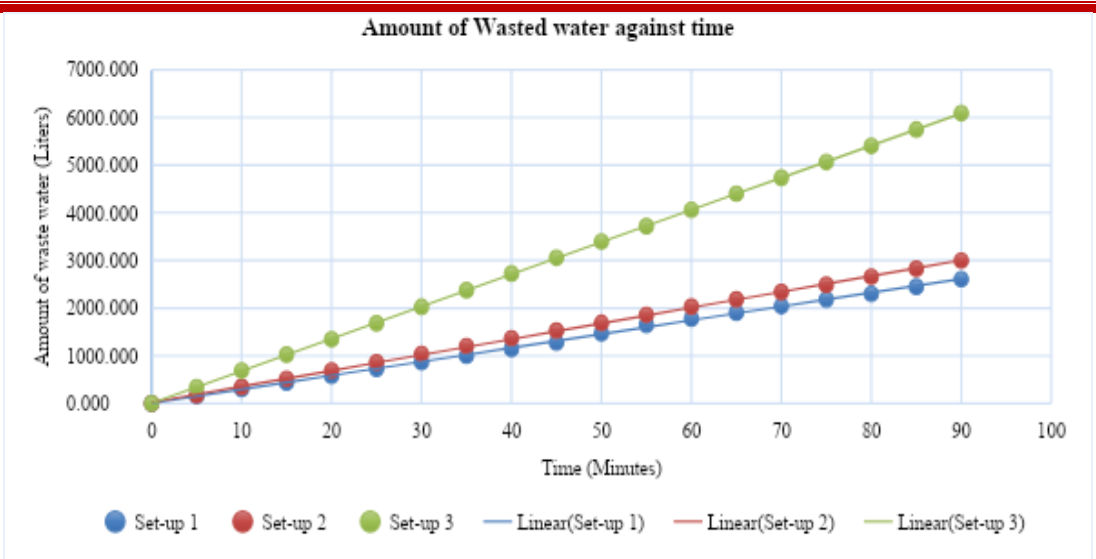


Figure 8: Amount of water wasted by the pump against time of the designed prototype hydram pump.

### 4) Discussion

Major cause of failure of the existing systems, was the imbalance of the pressure within the pump as a result of improper design of the valves and the pressure chamber. The efficiency of the pump depends on proper design of the valves and the pressure, since these are key controller of the pressures and the velocities of the system, which thereafter affects the pump's efficiency as observed by other workers (Kimaro, 2018).

The site conditions, drive and delivery heads and stream flows, are key components when installing the pumps. A similar observation was made by Asvapoositkul et al., (2019). The existing systems failed due to inadequate designs of the head ratio to flow ratio. The higher head ratio results to high pressure build up in the pump. This pressure is due to water hammer effect of the pump that causes a portion of water to be pumped to delivery tank (Inthachot, et al., 2015). The higher pressure generated in the pump can destroy the pump components, that is the valves, pressure chamber and pipes. Therefore, pressure chamber should be designed to absorb the pressure within the pump. This finding has been corroborated by Mishra et al, (2018).

### 5) Conclusions

Hydraulic ram pump has a great potential in providing alternative pumping solutions to rural population for domestic and agricultural use. The investigation carried out showed that hydram technology is well utilized in West Pokot County, Kenya. This is because it is cheaper and easy to fabricate and install as compared to motorized pumping systems.

The investigated systems, however performed with low efficiencies of below 30%. The study therefore, tries to sensitize and improve the locals' designed systems by providing a simplified designed prototype that can be used to develop new systems and also highlights on how they can improve their existing systems. From the study, the pump was able to achieve an optimum efficiency of 54% with optimum delivery flow rate of 12.938L/min, further studies can be carried out to improve the efficiency of the pump by modifying the pump, that is the valves and pressure chamber.

**Acknowledgement**

The work reported here was undertaken as part of the Building Capacity in Water Engineering for Addressing Sustainable Development Goals in East Africa (CAWESDEA) project which is part of the IDRC funded programme on Strengthening Engineering Ecosystems in sub-Saharan Africa. CAWESDEA Project is led by Global Water Partnership Tanzania in collaboration with Makerere University (Uganda), Moi University (Kenya) and University of Dar es Salaam (Tanzania).

**References**

1) Asvapoositkul, W., et. al. Determination of Hydraulic Ram Pump Performance: Experimental Results. Hindawi Advances in Civil Engineering, 1-12 (2019).
2) Harith, M. N, et al, M. A significant effect on flow analysis & simulation study of improve design hydraulic pump. IOP Conf. Series: Materials Science and Engineering, 1-14 (2017).
3) Hussin, N. S., et al. Design and analysis of hydraulic ram water pumping system. IOP Conf. Series: Journal of Physics, 1-9 (2017).
4) Inthachot, M., et al. Hydraulic ram pumps for irrigation in Northern Thailand. Agriculture and Agricultural Science Procedia 5, 107-114 (2015).
5) Januddi, F. S., et al. Development and Testing of Hydraulic Ram Pump (Hydram): Experiments and Simulations. Materials Science and Engineering, 1-8 (2018).
6) Kherde, A., et al. Research Paper on Hydraulic Ram Pump. Iconic Research and Engineering Journals, 282-284 (2020).

7) Kimaro, S. J. The Influence of Air Vessel Volume on the Delivery Flow Rate and Efficiency of a Hydram Water Pumping. International Research Journal of Engineering and Technology, 1312-1320 (2018).

8) Laxmi, N. S., et al. Performance Evaluation Hydraulic Ram Pump with Rain-Cum-Roof Water Harvesting Structure in Hilly Terrains of North East India. Journal of Agroecology and Natural Resource Management, 317-320 (2015).

9) Mishra, N., et al. Effect of Water Hammering Action on Performance of Hydraulic Ram Pump. International Journal of Scientific and Research Publications, 1-5 (2018).

10) Mohammed, S. N. Design and Construction of a Hydraulic Ram Pump. Leonardo Electronic Journal of Practices and Technologies, 1-5 (2019).

11) Ochieng, J., et al. Effects of climate variability and change on agricultural production: The case of small-scale farmers in Kenya. NJAS - Wageningen Journal of Life Sciences, 71-78 (2016).

12) Pawlick, M., et al. Ram pump design and installation: Manual for use in developing countries. Research Gate Journal, 1-5 (2018).

13) Rajaonison, A., & Rakotondramiarana, H. T. Theoretical Study of the Behavior of a Hydraulic Ram. American Journal of Fluid Dynamics, 1-12 (2019).

14) Sheikh, S., et al. Design Methodology for Hydram. International Journal of Mechanical Engineering and Robotics Research, 6 (2013).

15) Tacke, J. Hydraulic rams; a comparative investigation. Delft: TU Delft - Delft University of Technology (1998).

16) Than, P. M., et al. Performance Testing of a Hydraulic Ram Pumping. Iconic Research and Engineering Journals, 144-150 (2019).

17) Veljko, F., et al. Mathematical modelling of a hydraulic ram pump system. Journal of mechanical engineering, 137-149 (2003).

18) Verspuy, C., & Tijsseling, A. Hydraulic ram analysis. Journal of hydraulic research, 1-5 (1993).

19) Watt, S. B. A Manual on the Hydraulic Ram for Pumping Water. London: Intermediate Technology Publications Limited (1975).

# HVDC Opportunities for Achieving SDG7 for East Africa Region

J. D. Bwire[1*], J. N. Ouma[2], S. Opana[3].

[1] Kenya Power Company Kisumu, P.O Box 151-40100 Kisumu, Kenya

[2]State Department for Public Works Nairobi, P.O. Box 41191 – 00100 Nairobi, Kenya

[3]AUDA-NEPAD

Corresponding Author: Japhethbwire@gmail.com

**Abstract**

Globally, and especially in developing countries, the demand for electrical power is rising. Along with climate change concerns, the increase in demand has led to rapid expansion in generation especially from renewable energy sources. Consequently the existing energy infrastructure has been left struggling to cope with power transfer levels above their initial limits. The sub-Saharan region, including South Africa, has been highly affected by the critical challenges of load-shedding, which impedes economic growth and aggravates unemployment. One obvious solution to transmission congestion is to construct additional HVAC lines as seen across the region. However, apart from the capital costs, new rights of way require environmental impact and engineering assessments, a long list of licenses, agreements, authorizations and compulsory land purchases. Thus, power transmission companies need to look for alternative technologies that can enhance power transmission and integrate renewables while maximizing existing rights of way.

In a world consumed by cost-cutting yet obliged to improve environmental impact, HVDC is the answer to this challenge faced by energy companies: move more power, more efficiently, with the lowest losses possible. As envisioned by SDG7: access to reliable, affordable and clean energy to all. The paper using a case study of East Africa argues the Africa energy sector to consider converting existing HVAC to HVDC as opposed to developing new HVAC lines especially for interconnectors across neighboring countries. The paper highlights how this will increase the capacity thus ensuring that countries are able to share cheap RE, reduces power losses and improve reliability.

**Keywords:** HVDC, HVAC, SDG7, Power transmission, Grid Connection, interconnector.

## 1) Introduction

East Africa and Africa at large is characterized by dispersed loads and generation sources spanning hundreds and in some case thousands of kilometers. With electricity demand growing daily as experienced across the continent, there is urgent need for energy sector to plan and work around the clock on moving more power to the load centers. This will play a key role in attainment of Africa climate summit 2023 resolution of Increasing Africa's renewable generation capacity from 56 GW in 2022 to at least 300 GW by 2030, both to address energy poverty and to bolster the global supply of cost-effective clean energy for industry [1]. Bulk power transmission from generation stations to the load centers is transferred using high voltage network. High voltage alternating current (HVAC) has dominated the transmission of bulk power for a long time. Despite HVAC having a number of advantages some of its pitfalls which include; high power losses, relatively lower power transfer capacity and prone to stability challenges. Therefore, to urgently address the aforementioned challenges associated with HVAC, most energy sectors are opting to use HVDC lines in this era of green energy, which are site specific, and for attainment of SDG7. HVDC power lines possess many advantages over HVAC lines in economics, high power transfer capacity, system stability, reliability, control, low short circuit current levels, structural simplicity, and low line power losses [2].

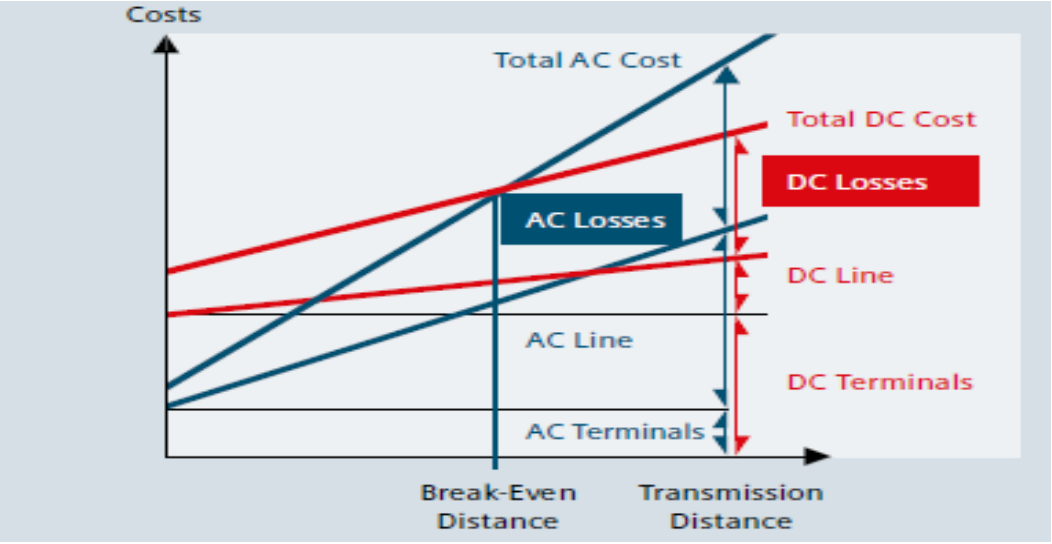


Fig.1. Comparison of Cost vs Distance between HVAC and HVDC [3].

A number of studies have shown that conversion of HVAC lines to HVDC lines increases the power transmission capability [2]. This fact lets the conversion HVAC to HVDC as an interesting alternative for the Transmission Expansion Planning, TEP, even more if

restrictions to build new lines are more demanding. With East African countries struggling with the transfer of more power on the aging transmission infrastructure, HVDC offers a solution to the highlighted challenges. A DC transmission line has a lower visual profile than an equivalent AC line and so Contributes to a lower environmental impact. There are other environmental advantages to a DC transmission line through the electric and magnetic fields being DC instead of AC.

Different lay-outs can be applied for the considered HVDC link, such as a monopolar or bipolar system with ground return or metallic return. A bipolar system with ground return is chosen as it offers increased redundancy and allows some flexibility for future tappings/extensions. The increased redundancy is achieved because the system can still operate at 50% of its nominal rating in case of an outage of one converter or line. HVDC links not only decouple both HVAC systems such that faults in one system do not propagate to the other system, they can also provide grid support after an incident takes place. One of such support mechanism, which would be of interest, is to provide frequency control to the EAPP system. Countries with substantial amount of inertia and primary reserve can be offered to the systems by modifying the power controllers.

The paper proposes to the African energy sector to consider conversion of the existing HVAC to HVDC as opposed to developing new HVAC lines especially for interconnectors across neighboring countries. The paper highlights how this will increase the capacity thus ensuring that countries are able to share cheap RE, reduces power losses and improve reliability as they work towards attainment of SGD7 and Vision 2030/2063.

### 2) Conversion of HVAC to HVDC Transmission Lines.

The conversion of HVAC lines to HVDC is an interesting alternative recently analyzed and currently has very few cases implemented globally. Several feasibility studies for conversion of lines describe the main aspects to take into account to increase the transmission capability. Two types of line's conversion are proposed [2]:

Table 1: proposed line conversion methods

| **Type A:** | **Type B:** |
|---|---|
| Minor modifications in the structure that can be performed by changing the allowable height of the conductors with respect to ground during the conversion process. | Major modifications of structures that do not allow conductors can be located at a suitable distance from ground during the conversion process. |

Type A conversion could consider hot-line work to reduce the downtime of the line. This can be a key factor to reduce the impact on the reliability of the transmission system during the conversion process. Conversion Type B may require that the line remain out of service for extended periods, thus having a greater impact on the reliability of the system. However, the increase in transmission capacity can be higher than Type A conversion.

Table 2: shows the results of expected capacity on conversion type to be used [4, 5].

| HVAC AC double circuit | Rated MW | HVDC Bipolar Topology Technology | Mw Expected | Percentage Increment | Conversion Type |
|---|---|---|---|---|---|
| 145kV | 110 | $\pm 290kV$ | 390 | 255% | Type B |
| 245kV | 380 | $\pm 490kV$ | 1,330 | 250% | Type B |
| 520kV | 990 | $\pm 840kV$ | 3,430 | 246% | Type B |
| 420kV | 1,200 | $\pm 400kV$ | 2,200 | 83% | Type A |
| 287kV | 560 | $\pm 240kV$ | 863 | 54% | Type A |
| 287kV | 560 | $\pm 245kV$ | 1,762 | 215 | Type A |

The conversion of HVAC lines to HVDC reduces both the cost of investment and the Break Even Distance (BED). Conversion of lines extends the distance range in which the HVDC is less expensive than HVAC for transmission lines.

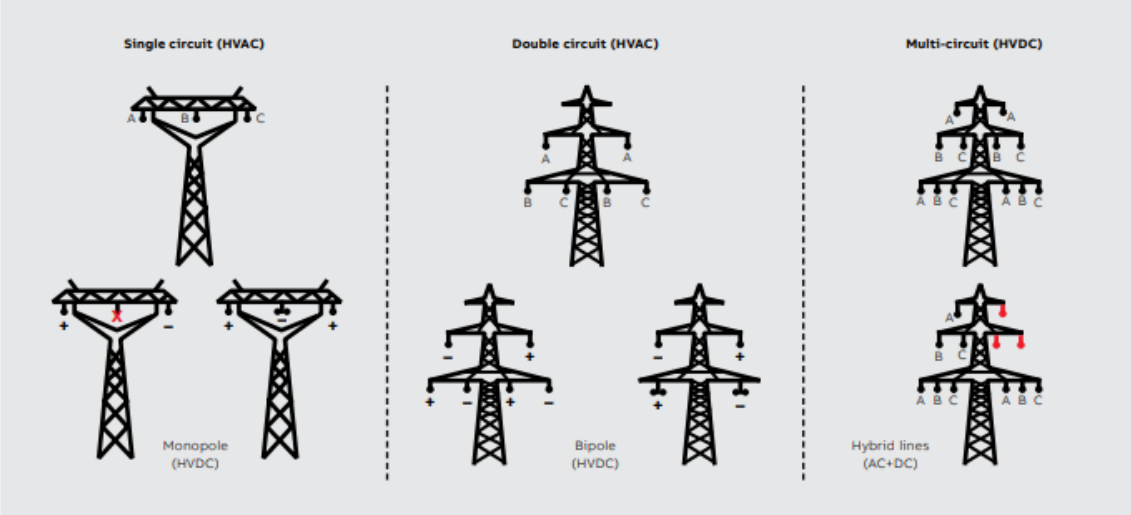


Fig2. Converting HVAC to HVDC towers

### 3) Methodology

In this study, two options were considered with the focus area on Lake Turkana Wind Power Plant (LTWP) to Suswa transmission corridor. The paper assumed that LTWP to Suswa is energized and operated at 400kV AC as designed. The methodology used two stages in each of the analyzed options: The computation of power losses from the transmitted power and the assessment of maximum transfer capacity of the transmission lines. The transfer capacities in both options were computed by carrying out the PV analysis and power losses were approximated by running load flow simulations. Modeling and simulations were done on Power System Simulator for Engineering (PSS/E) version 33 (see Fig. 3 and 4).

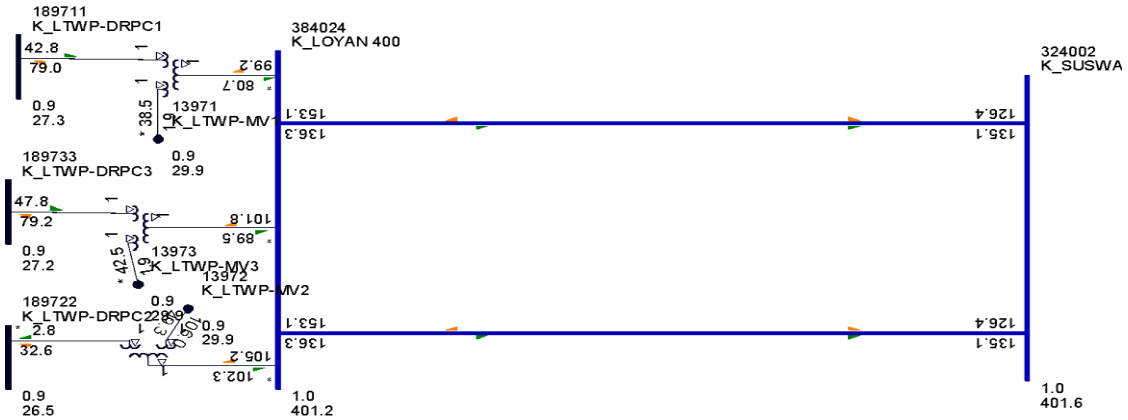


Fig. 3: HVAC for LTWP-Suswa 400kV

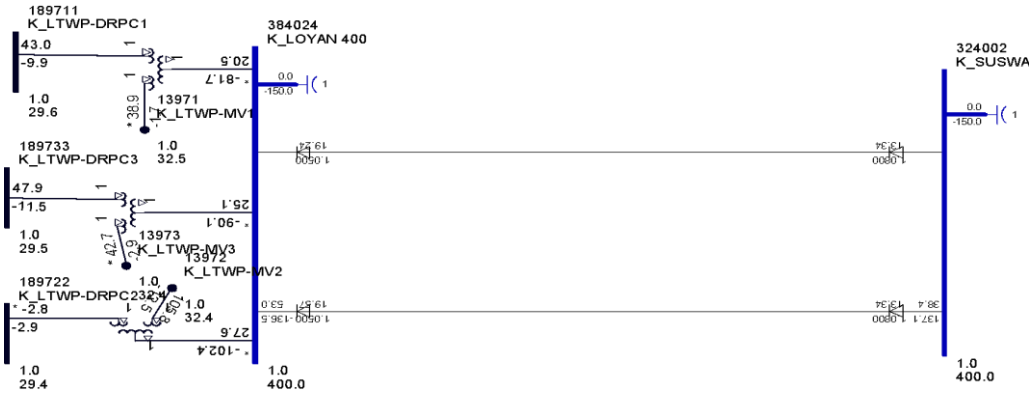


Fig. 4: HVDC for LTWP-Suswa 500kV

### 4) Results and Discussions

The load flow and maximum transfer capacities calculated for HVAC and HVDC systems are as shown in Table3. Fig.3 indicates that maximum transfer capacity calculated for LTWP-Suswa 400kV HVAC lines was 2360MW with the rated capacity of 3275.6MVA whereas the transfer capacity for the simulated LTWP-Suswa 500kV

HVDC was 3000MW equivalent to the rated capacity of the lines of 3000MVA. The difference in the power carrying capabilities between HVAC and HVDC arises because the transmission capacity of HVAC operates based on its operational security (voltages at the notes) and reactive power, whereas HVDC is only limited by the thermal constraints associated with the conductor. Therefore, it can that deduced that conversion of a transmission line from HVAC to HVDC might provide improved transmission capacity and reduced transmission losses.

Table 3: shows the results of capacity increase on conversion type A to be used.

| **HVAC AC double circuit** | **Rated MW** | **HVDC Bipolar Topology Technology** | **Mw Expected** | **Percentage Increment** | **Conversion Type** |
|---|---|---|---|---|---|
| 400kV | 2360 | $\pm 500kV$ | 3000 | 127.11% | Type A |

## Cost Analysis

A first basic cost estimation of the presented HVAC and HVDC options are presented for a direct connection between LTWP and Suswa. This paper considered investment calculation costs. Furthermore, the cost of the AC substations, which have to be built for all studied options, are not included. Therefore, the costs as given are merely to compare the different options and give not a good estimate of the final cost.

Table 4: cost comparison for HVAC VS HVDC

| **HVAC line (400 kV)** | **HVDC line (VSC - 1GW – without intermediate tapping)** |
|---|---|
| Lines + compensation (400 kV double circuit)= 1.5×430 km×0.40 M$ = 258 M$<br>(Additional substations used for voltage control (2): 64.4 M$)<br>Approximate total cost of double circuit<br>=USD 322.4M | Converter stations = 2*144 M$ = 288 M$<br>Bipolar Lines = 430 km*0.29 M$ = 362.5 M$<br>Approximate total cost for bipolar converter station<br>=USD 387.0M |

Thus;

Annual cost of the power Losses

Difference in the losses between HVAC and HVDC

=4.08MW-1.1MW

=2.98MW

It is possible to establish a relationship between peak demand on a system and the average technical losses through consideration of load factors and loss load factors. Load factor (LF) is the ratio of the average demand over a period to the maximum demand within that period for the particular network and loss load factor (LLF) is the as average power losses over a period to the losses at the time of peak demand.

The formula adopted is:

$$LLF = (0.3 \times LF)+( 0.7\times LF\times LF) \quad \text{……..(1)}$$

As the basis for loss calculations, because the network considered is mainly transmission. Using the LLF formula stated and an assumed load factor of 0.693;

Thus:

$LLF = 0.3 \times LF + 0.7 \times LF^2$

$LLF = 0.3 \times 0.694 + 0.7 \times 0.694^2$

$LLF = \underline{0.545}$

Annual energy losses (kWh)

$$\text{Power Losses (kW)} \times LLF \times 8760\text{hrs} \quad \text{…… (2)}$$

Thus: $=2980\times0.545\times8760$

$\cong 14{,}227{,}116\text{kWh}$

Using data from EPRA which indicates that the average energy cost (excluding the capacity costs) in April 2022 was 10.36kshs/kWh [6], therefore, the cost benefit on the power losses gained by implementing HVDC is:

Cost on energy losses saved = 14,227,116kWh×10.36kshs/kWh

$\cong$Ksh. 147.392M

From the analysis, it's clear that HVDC offers high power transfer capacity and lower power losses compared to HVAC even though the HVDC has high investment costs. However, the high investment cost is offset by the cost saved on the high-energy losses likely to be experienced with HVAC.

## 5) Conclusion

Based on the result of this paper with other preceding papers, the utilities within EAPP should consider the implementation of hybrid HVAC/HVDC system. By doing so, the utility company will save on cost, increase transmission efficiency and reduce socio-economic problem emanating from resettlement programs. Therefore, we recommend the use of HVDC transmission lines in evacuation of power form the isolated wind and solar generation plant which are oftentimes site specific, this will ensure reduced losses as these plants are normally far away from load center thus optimization of the green energy transition and attainment of SDG7.

**References:**

[1] The_african_leaders_nairobi_declaration_on_climate_change-rev-eng; 2023

[2] A. Clerici, L. Paris, and P. Danfors, "HVDC conversion of HVAC lines to provide substantial power upgrading," *IEEE Transactions on Power Delivery*, vol. 6, no. 1, pp. 324-333, Jan. 1991.

[3] www.siemens.com/energy/hvdc:

[4] J. Lundkvist, I. Gutman, and L. Weimers, "Feasibility study for converting 380 kV AC lines to hybrid AC / DC lines," in *EPRI High-Voltage Direct Current & Flexible AC Transmission Systems Conference*, Westminster, USA, Nov. 2009, pp. 1-25.

[5] M. Beshir, L. Barthold, and D. Woodford, "Prospective AC to DC conversion of two parallel 287 kV transmission lines in the Western US," in *Proc. CIGRE Session 44*, Paris, France, 2012.

[6] Energy and Petroleum Regulatory Authority (EPRA) – Integrates Annual Report and Financial Statements for the years ended 30th June 2021 and 30th June 2022.

## Editorial Committee



## Editorial Board

# INSTRUCTIONS TO CONTRIBUTORS

The editorial staff of the AJERI requests contributors of articles for publication to observe the following editorial policy and guidelines accessible at https://www.iekenya.org/ in order to improve communication and to facilitate the editorial process.

## Criteria for Article Selection

Priority in the selection of articles for publication is that the articles:

a. Are written in the English language
b. Are relevant to the application relevant of engineering and technology research and Innovation
c. Have not been previously published elsewhere, or, if previously published are supported by a copyright permission
d. Deals with theoretical, practical and adoptable innovations applicable to engineering and technology
e. Have a 150 to 250 words abstract, preceding the main body of the article
f. The abstract should be followed by a list of 4 to 8 "key Words"
g. Manuscript should be single-spaced under 4,000 words (approximately equivalent to 5-6 pages of A4-size paper)
h. Are supported by authentic sources, references or bibliography

## Rejected/Accepted Articles

a. As a rule, articles that are not chosen for AJERI publication are not returned unless writer (s) asks for their return and are covered with adequate postage stamps. At the earliest time possible, the writer (s) is advised whether the article is rejected or accepted.
b. When an article is accepted and requires revision/modification, the details will be indicated in the return reply from the AJERI Editor, in which case such revision/modification must be completed and returned to AJERI within three months from the date of receipt from the Editorial Staff.
c. Complementary copies: Following the publishing, three successive issues are sent to the author(s)

## Procedure for Submission

a. Articles for publication must be sent to AJERI on the following address:

*The Editor*

*African Journal of Engineering Research and Innovation*

*P.O Box 41346- 00100*

*City Square Nairobi Kenya*

*Tel: +254 (20) 2729326, 0721 729363, (020) 2716922*

*E-mail: editor@iekenya.org*

b. The article must bear the writer (s) name, title/designation, office/organization, nationality and complete mailing address. In addition, contributors with e-mail addresses are requested to forward the same to the Editor for faster communication.

For any queries, authors are requested to contact by mail (editor@iekenya.org).

**PUBLISHER**

The Institution of Engineers of Kenya (IEK)

P.O Box 41346- 00100

City Square Nairobi Kenya

Tel: +254 (20) 2729326, 0721 729363, (020) 2716922

Email: editor@iekenya.org

Website: www.iekenya.org

**CONTENTS** **Pages**